UNIVERSIDADE DE SÃO PAULO
FACULDADE DE ODONTOLOGIA DE BAURU

RICARDO QUÍRICO PINHEIRO MACHADO

Pre-clinical and clinical studies of a novel porous biphasic calcium phosphate ceramic as alternative to repair bone defects

Estudos pré-clínico e clínico de uma nova cerâmica bifásica porosa de fosfato de cálcio como uma alternativa para o reparo de defeitos ósseos

BAURU
2018

RICARDO QUÍRICO PINHEIRO MACHADO

Pre-clinical and clinical studies of a novel porous biphasic calcium phosphate ceramic as alternative to repair bone defects

Estudos pré-clínico e clínico de uma nova cerâmica bifásica porosa de fosfato de cálcio como uma alternativa para o reparo de defeitos ósseos

Tese constituída por artigos apresentada a Faculdade de Odontologia de Bauru da Universidade de São Paulo para obtenção do título de Doutor em Ciências no Programa de Ciências Odontológicas Aplicadas, na área de concentração Biologia Oral.

Orientadora: Prof.ª Dr.ª Marília Afonso Rabelo Buzalaf

BAURU
2018

Machado, Ricardo Quírico Pinheiro Machado

Pre-clinical and clinical studies of a novel porous biphasic calcium phosphate ceramic as alternative to repair bone defects / Ricardo Quírico Pinheiro Machado. – Bauru, 2018.

113p.; il; 30cm.

Tese (Doutorado) – Faculdade de Odontologia de Bauru. Universidade de São Paulo

Orientadora: Prof.ª Dr.ª Marília Afonso Rabelo Buzalaf

Comitê de Ética da FOB-USP
CAAE: 03625812.1.0000.5417
Parecer Número: 139.405
Data: 31/10/2012

FOLHA DE APROVAÇÃO

DEDICATÓRIA

Dedico este trabalho à minha esposa e filha, Amanda Inri Cella Pinheiro Machado e Nadine Cella Pinheiro Machado

AGRADECIMENTOS

À minha orientadora ***Profa. Dra. Marília Afonso Rabelo Buzalaf***.

Aos meus pais, ***Roberto Pinheiro Machado*** e ***Christina Quírico Pinheiro Machado***.

Aos meus amigos, colegas e pós-graduandos do Departamento de Ciências Biológicas da Faculdade de Odontologia de Bauru, Universidade de São Paulo.

Aos professores, técnicos e funcionários do Departamento de Bioquímica e Histologia da Faculdade de Odontologia de Bauru, Universidade de São Paulo.

Em especial ao ***Prof. Dr. Eulazio Taga, Prof. Dr. Rumio Taga, Dra. Tania Maria Cestari, Dalva Ribeiro de Oliveira, Prof. Ever Elias Mena Laura*** e ***Ana Carolina Cestari Bighetti.***

AGRADECIMENTOS INSTITUCIONAIS

Ao ***Prof. Dr. Vahan Agopyan***, digníssimo Reitor da Universidade de São Paulo.

Ao ***Prof. Dr. Pedro Vitoriano Oliveira***, digníssimo secretário Geral da Universidade de São Paulo.

Ao ***Prof. Dr. Carlos Ferreira dos Santos***, digníssimo Diretor da Faculdade de Odontologia de Bauru da Universidade de São Paulo.

Ao ***Prof. Dr. Guilherme dos Reis Pereira Janson***, digníssimo Vice-Diretor da Faculdade de Odontologia de Bauru da Universidade de São Paulo.

Ao ***Prof. Dr. José Roberto Pereira Lauris***, digníssimo Prefeito do Campus da Faculdade de Odontologia de Bauru da Universidade de São Paulo.

À ***Profa. Dra. Izabel Regina Fischer Rubira Bullen***, digníssima Coordenadora do Programa de Pós-Graduação em Ciências Odontológicas Aplicadas e Presidente da Comissão de Pós-Graduação na área de Estomatologia e Biologia Oral, da Faculdade de Odontologia de Bauru da Universidade de São Paulo.

“What we do in life, echoes to eternity”

— Gladiator (2000)

ABSTRACT

Objectives: We compared a novel porous biphasic calcium phosphate (pBCP) containing 70% HA and 30% β-TCP with autogenous bone (AB) regarding bone formation, graft granular size influence (0.7, 1.0 or 1.5 mm), physicochemical properties, and volumetric changes of the total grafted area as well its components (newly formed bone, graft particle stability and soft tissue). **Materials and methods:** Article 1 used a critical size defect in rats. Analyzes included XRD (X-ray diffraction), SEM (scanning electron microscope) and EDS (Energy-dispersive X-ray spectroscopy) *in vitro* and then histomorphometry of biopsies collected from rat skull. Article 2 used a bilateral MSFA by lateral wall surgery in 12 patients in a split-mouth design. Analyses of three-dimensional (3D) cone beam computed tomography (CBCT) scans at different periods (T0, T1 and T2), and of micro-CT scans and histological slides of graft core biopsies were performed. **Results:** In the preclinical approach, similar physicochemical characteristics among pBCPs with different granular sizes were found. Besides, osteopromotion regarding pBCP granular sizes of 0.7 and 1.0 were higher than AB. In the clinical approach, pCBP was similar to AB. However, in both approaches, the volume of the total grafted area and particles within the grafted area were more reduced for AB (45% and 37%, respectively, in article 1 and 31% and 33%, respectively, in Article 2). For pBCP these volumetric changes did not occur, except for 1.5 mm size group in the preclinical approach, which showed a significant reduction in the last period (24 weeks). **Conclusion**: pBCP70:30 physicochemical characteristics, such as slow resorption, creates a favorable microenvironment for bone formation that is directly influenced by the granule size. pBCP70:30 promotes greater preservation of the grafted volume than AB, thus being a good alternative for MSFA and bone regeneration procedures.

Keywords: Bone substitutes;Bone regeneration; Maxillary sinus; X-Ray Microtomography; Histology

RESUMO

Objetivos: Nós comparamos um novo fosfato de cálcio bifásico poroso (pBCP contendo 70% HA e 30% β-TCP com o osso autógeno (AB) quanto à formação óssea, influência do tamanho granular do enxerto (0,7, 1,0 ou 1,5 mm), propriedades físico-químicas e alterações volumétricas da área total enxertada, bem como seus componentes (osso recém-formado, estabilidade das partículas do enxerto e tecido mole). MATERIAIS E MÉTODOS: O artigo 1 usou um defeito de tamanho crítico em ratos. As análises *in vitro* incluíram XRD (difração de raios X), SEM (microscopia eletrônica de varredura) e EDS (espectroscopia de dispersão de energia por raios X) e depois análise histomorfometria de biópsias coletadas da calvária de ratos. O artigo 2 envolveu utilização do material para elevação bilateral de seio maxilar em 12 pacientes, em um desenho *split-mouth*. Análise de tomografia computadorizada tridimensional (3D) de feixe cônico (TCFC) em diferentes períodos (T0, T1 e T2), micro-CT *scans* e lâminas histológicas de biópsias do enxerto foram realizadas. Resultados: Na abordagem pré-clínica, foram encontradas características físico-químicas semelhantes entre os pBCPs com diferentes tamanhos granulares. Em adição, a osteopromoção, para os tamanhos granulares do pBCP de 0,7 e 1,0 mm foram maiores que para o AB. Na abordagem clínica, o pBCP foi semelhante ao AB. No entanto, em ambas as abordagens, o volume total da área enxertada e o volume das partículas dentro da área enxertada foram menores para o AB (45% e 37% respectivamente no artigo 1 e 31% e 33% respectivamente no Artigo 2). Para o pBCP mudanças volumétricas não ocorreram, exceto para o grupo tamanho 1,5 mm na abordagem pré-clínica, que mostrou uma redução significativa no último período (24 semanas). Conclusão: As características físico-químicas do pBCP, como a lenta reabsorção, criam um microambiente favorável para a formação óssea e isso é diretamente influenciado pelo tamanho dos grânulos. O pBCP70: 30 promove maior preservação do volume enxertado em comparação ao AB, sendo uma boa alternativa para o aumento do seio maxilar e para os procedimentos de regeneração óssea.

Palavras-Chave: Substituos ósseos; Regeneração óssea; Seio Maxilar; Microtomografia por Raio-X; Histologia

TABLE OF CONTENTS

1 INTRODUCTION

1 INTRODUCTION

Bone grafting aims to replace missing bone in complex areas where bone reposition or healing fails. It is achievable due to the bone tissue capacity to regenerate completely if sufficient space is provided into which it has to grow. In orthopedic and maxillofacial surgery fields, various types of biomaterials are being used for bone repair and regeneration procedures (Jordana *et al.*, 2017). The development and modification of these materials seek to improve the speed and quality of healing (Ebrahimi *et al.*, 2017), since in Dentistry, there are different clinical situations that need biomaterials with specific characteristics or properties.

Concerning bone grafting and substitute materials, for many years autogenous bone (AB) has been the first biomaterial of choice, since it has the three main properties of a bone grafting substitute including osteoconductivity, osteoinductivity and osteogenicity. Autogenous bone grafts, besides its unique natural three-dimensional structure and host cells, contain growth factors and promote the recruitment of new stem cells. Therefore, AB is currently the "gold standard" in bone grafting. These three main properties are determined by the chemical composition, cells and the physical structure of the biomaterials (Daculsi *et al.*, 2013). n case of AB, the amount of graft is very limited, the removal of intraoral bone increases the surgical time and the morbidity of the donor site, and it represents another potential local for postoperative pain and complications.

Due to these disadvantages, many bone substitutes have been developed in laboratory with materials from extracted humans, animals and synthetic sources. In Dentistry, bone grafts are used as fillers and scaffolds to facilitate bone formation during wound healing (Polo-Corrales *et al.*, 2014). The grafts should be bioresorbable and have no antigenic

properties. For example, bone allografts and xenografts are recognized by the recipient's immune system as foreign and will therefore be attacked in a process termed rejection (Shibuya and Jupiter, 2015). Additionally, the grafts should act as a mineral reservoir, which in turn induces new bone formation. Accordingly, there is a variety of bone substitutes classified by the origin or the type of material used on their production. It includes allografts, synthetic variants, xenografts, growth factors, alloplastic grafts, ceramic based grafts, polymer-based grafts and cell based grafts (Kumar *et al.*, 2013). Some of them have shown good rate of success and are widely accepted and supported by literature, however availability and cost could be still a disadvantage (Wang and Yeung, 2017).

Ceramic based-bone substitute grafts include calcium phosphate, calcium sulphate, and bioglass used alone or in combination. Most of the materials present a single phase then they are referred as monophasic, that is seen in hydroxyapatite (HA) bioceramics. Thus, terms such as biphasic and multiphasic are used for bioceramics having two or more compounds with similar physical properties (Dorozhkin, 2012). Tricalcium phosphate was originally presented as a single phasic material until it was found that it had 20% of HA and 80% of tricalcium phosphate TCP (Ebrahimi *et al.*, 2017). HA is a natural compound of the mineral phase of bone; therefore it has good biocompatibility and, additionally, it is more stable and has better mechanical properties than α- and β-TCP (Dorozhkin, 2012; Bouler *et al.*, 2017; Ebrahimi *et al.*, 2017). HA is most often combined with β-TCP because of its higher stability and lower solubility than α-TCP (Vereecke and Lemaître, 1990; Chow, 1991). Furthermore, β-TCP induces more bone formation in mesenchymal stromal cells than HA (Yuan *et al.*, 2010; Prins *et al.*, 2016). Indeed, the combination of HA with TCP is the most studied material among bone ceramics, since this combination forms a bioactive compound with good grafting properties. Efforts to obtain a bone substitute with favorable properties and suitable for MSFA are still being done. Attention has grown for BCPs scaffolds for having not only

osteoconductive but also osteoinductive properties, even when implanted heterotopically (Coathup *et al.*, 2012). In this respect, article 1 approaches the use of porous HA/TCP 70/30 in MSFA in patients compared to autogenous bone with a 6-month period of healing prior to implant placement.

BCPs may also show some drawbacks such as poor mechanical strength, lack of collagen or other organic compounds, presence of impurities, micro-scale grain size and non-homogenous particle size and shape. However, in the last years, several changes on the production parameters such as sintering temperature, sintering soaking time, pH and purity of the initial materials, have given rise to biomaterials with improved physicochemical properties regarding specific surface area, surface energy, surface charge, surface topography and roughness, grain size and porosity (Daculsi and Legeros, 2006; Zhang *et al.*, 2018). Porosity has called attention due to particular situations, as for example, it was reported that bone did not form in ceramics lacking microporosity, additionally, the osteoinduction potential seems to increase with their presence (Habibovic *et al.*, 2005; Hing *et al.*, 2005; Yuan *et al.*, 2010; Coathup *et al.*, 2012). The macroporosity also potentiates the osteoinductive capacity of microporous structures (Habibovic *et al.*, 2005; Coathup *et al.*, 2012). Recently, Wang et al. (2015) pointed out that porosity has a direct relation with the particle size. In this regard, different outcomes were obtained on the studies comparing particle size of bone ceramics in its efficiency on bone repair (Coathup *et al.*, 2013; Wang *et al.*, 2015) therefore an optimal mean size for BCP particles for clinical use is still inconclusive. It should be noted that in addition to the particle size, all physicochemical configurations of bone substitutes directly influence the host response to bone grafting (Chen *et al.*, 2015).

In an attempt to approach the role of the particle size of BCPs on the healing and regeneration of the bone defects, we performed a second preclinical and complementary

experimental research. The article 1 uses the critical size cranial defect model in rats to test different particle size of the porous HA/TCP-70/30. Few studies exist on the effect of BCP particle size on healing and regeneration of critical-size bone defects and the outcomes are diverse. We hypothesized that particle size variation may influence the bioactivity of the biomaterial as well as the host healing response.

Atrophy of the alveolar bone is aggravated by tooth loss in a chronic, progressive and irreversible way (Bodic *et al.*, 2005). Losing bone by pneumatization of the maxillary sinus is another condition that occurs with aging in both dentulous and edentulous individuals. However, it is more intense in cases of loss of two or more teeth and alveolar atrophy in the posterior region. In these cases, immediate implant placement or immediate bone grafting is indicated (Sharan and Madjar, 2008). For implant placement, host factors such as the residual amount of the bone, quality of the bone, patient's overall condition, local environment and anatomical variability can affect implant success (Martin *et al.*, 2009; Chrcanovic *et al.*, 2017). Therefore, rehabilitation of these patients by use of dental implants remains a challenge in Dentistry.

To overcome these issues, bone augmentation in posterior maxilla is performed with different surgical techniques and the most used are alveolar ridge augmentation and maxillary sinus floor augmentation. Alveolar ridge augmentation is less invasive and within its category are other techniques such as, guided bone regeneration (GBR), onlay/veneer grafting (OVG), combinations of onlay, veneer, interpositional inlay grafting (COG), distraction osteogenesis (DO), ridge splitting (RS), free and vascularized autografts for discontinuity defects (DD), mandibular interpositional grafting (MI), and socket preservation (SP) (Aghaloo and Moy, 2007; Mcallister and Haghighat, 2007). They show good rate of success, however alveolar bone augmentation by maxillary sinus floor augmentation is the most successful method

because it resolves vertical dimension's deficiency, which is the major challenge for implant placement (Aghaloo and Moy, 2007).

Maxillary sinus floor augmentation (MSFA) has begun in the 60`s, particularly, to obtain a correct maxillary ridge and ideal vertical dimensions for prothesis making (Boyne and James, 1980). After that time, sinus floor augmentation was used in combination with dental implants. Currently, there are two techniques to approach the sinus cavity, the transalveolar approach and the lateral window approach (Caldwell-Luc technique) (Mohan *et al.*, 2015). The choice mainly depends on the alveolar residual ridge height (RRH) (Pal *et al.*, 2012). The lateral window approach technique to be used in combination with autogenous bone graft was first described by Tatum and published by Boyne and James in 1980 (Boyne and James, 1980). In 1988, two clinical cases using autogenous bone harvested intraorally and placed within the sinus were reported. Six months later, the implants were placed (Wood and Moore, 1988). Since then, the maxillary sinus floor augmentation is being performed for grafting with the intention of returning the height and width of the bone with a high degree of success (Dongo *et al.*, 2018). The success comes from the fact that it is simple technique, allows ideal blood irrigation, makes it difficult surgical contamination and allows the possibility of grafting large quantities of bone substitutes with a favorable postoperative healing. In article 2, we investigate bone regeneration and its volumetric stability after MSFA of the atrophied maxilla treated with novel porous biphasic calcium phosphate (pBCP70:30) in comparison with AB.

Thus, the general approach of these two studies is to evaluate the performance of a new porous BCP termed as pBCP70/30 in animal and human models. In both studies, factors such as time of healing, new bone formation and bone stability are assessed. They are relevant issues for MSFA, implant placement and other grafting purposes. Still there is scarce knowledge regarding bone substitutes to be used during MSFA and other medical-dental

procedures. The outcomes provided in these studies are helpful and provide new strategies in the bone regeneration and reconstruction field.

2 ARTICLES

2 ARTICLES

This thesis comprises two articles:

ARTICLE 1 – Influence of biphasic calcium phosphate particle size on the repair of cranial critical-size bone defects

ARTICLE 2 – Porous biphasic calcium phosphate ceramic for maxillary sinus floor augmentation: a randomized controlled clinical trial with CBCT, micro-CT and histomorphometry studies

2.1 ARTICLE 1 – Influence of biphasic calcium phosphate particle size on the repair of cranial critical-size bone defects

ABSTRACT

The diversity of tissue responses achieved in porous biphasic calcium phosphate (pBCP) materials are a consequence of their chemical and physical structures. Thus, physicochemical properties of a novel pBCP were determined by XRD (X-ray diffraction), SEM (scanning electron microscope) and EDS (Energy-dispersive X-ray spectroscopy). Subsequently, the bone repair efficacy of this pBCP with different granule sizes [small (pBCP0.7), medium (pBCP1.0) or large (pBCP1.5)] was evaluated in a standardized 8 mm critical size bone defects in rat skulls, comparatively to particulated autogenous bone (AB), by histomorphometry. For all pBCPs, the proportion between HA and β-TCP was of 70:30 and the surface showed small concavities and microporosities. Histologically, no significant reduction of pBCP, regardless the granule size, was observed and the presence of concavities on pBCP favored bone formation. At 4 weeks AB treatment was superior to pBCPs, promoting a higher bone gain (32.6±6.4 mm^3 vs. 12.27±3.79 mm^3). However, between 4 and 24 weeks, a higher reduction of AB particles and bone gain was observed in AB (BV=18.05 mm^3), while in pBCP0.7 and pBCP1.0, bone volume significantly increased by 175% (BV=34.668 mm^3). A significant reduction in bone gain was verified in pBCP1.5 (BV=22.57 mm^3), when compared to other granulation sizes. We concluded that the presence of concavities in pBCP surface associated to its slow absorption creates a favorable microenvironment for bone formation, which is directly influenced by the granule size. Thus, pBCP might be an efficient bone substitute to repair large bone defects, as an alternative to AB.

Keywords: Biphasic calcium phosphate; Physical chemistry characterization; Bone repair; preclinical animal model; critical size bone defect

INTRODUCTION

Introduction of calcium phosphate ceramics as bone substitutes represents one of the major advances in biomaterials science for the treatment of critical bone defects. The biphasic calcium phosphate (BCP) ceramics are composed of a steadier phase hydroxyapatite (HA), [$Ca_{10}(PO4)_6(OH)_2$], and a more soluble phase beta-tricalcium phosphate (β-TCP), [$Ca_3(PO4)_2$]. The preferential dissolution of the β-TCP component in the bone defect environment influences the bioreactivity of the biomaterial, which is inversely proportional to its HA/β-TCP ratio[1]. Thus, HA/β-TCP ratio variations, called crystallinity variations, influences their bioactivity and biodegradation, and determinates the biomaterial stability during conduction of osseous growth[2], advantages that favor their clinical use in oral and orthopaedic surgery. An ideal HA/β-TCP balance may also enhance mechanical strength and biological behaviors of these scaffolds[1].

However, the test of different HA/β-TCP ratios in different experimental situations has shown divergent results. In alveolar osseous defects, 85/15 and 65/35 ratios showed major attachment level gain than 50/50, 100/0, and 0/100[3]. In calvarial bone defects, a 60/40 ratio also showed greater bone formation than 0/100 at 4 and 8 weeks experimental periods[4]. Contrarily, other studies highlight the benefits of more β-TCP content in the biomaterial. Thus, 15/85 ratio showed a greater osteoinductive potential than 85/15, with faster and greater quantity of bone formation[5]. Additionally, it was reported that 30/70 and 20/80 ratios displaying faster graft resorption, more bone formation and space maintenance at 8 weeks[6]. While comparing different BCPs to the pure β-TCP *in vivo*, both high 60/40 and low 20/80 proportions HA/β-TCPs presented larger bone formation at 2 and 8 weeks with similar pattern of healing and particles biodegradation regarding the augmented area of bone[7]. Thus, it is possible to observe that there is still a lack of standardized BCP proportions for the vast clinical situations. The BCP osteoinductive activity linked to their physicochemical and three-

dimensional structural properties also has been reported [8,9]. In ours previous study, a novel synthetic porous BCP (pBCP) with 70:30 ratio was able to stimulate specific cellular responses in different microenvironments generated into rabbit mandibular bone defects, leading to new bone and cementum-like tissue formations[10].

In order to explore all these beneficial characteristics of a new biomaterial, the crucial first step in its biological evaluation process is the proper material characterization[11]. Many of the different properties of the material can be evaluated, but due to the complex biological responses to BCPs, the extent of this evaluation relies on the type of material and on the properties (osteoconduction, osteoinduction, osteogenesis) to be analyzed. According to Ebrahimi et al, 2017 [2], XRD, SEM and TEM analyses should be an integral part of material characterization in all types of BCP studies, especially in *in vivo* models. Besides, a scientific report should include details such as scaffolds' dimension, particle or granule size and crystal size and shape[12]. Regarding influence of the size of biomaterial particles in their osteogenic potential, studies are scarce and diverse. Thus, Coathup et al. (2013)[21], studying silicate-substituted calcium phosphate (SiCaP) particles with size among 1000–2000 μm, 90–125 μm and 90–125 μm, suggested that ceramic particles with 250–500 μm are more osteoconductive. For Pallesen et al. (2002)[13], autogenous bone with particles measuring 0.5 to 2 mm^3 is better than those measuring 10mm^3 for grafting procedures. Barbeck et al. (2015)[14], using biphasic phosphate ceramics between 400-1000 μm reported no influence of granules size in resorbing cells recruitment.

The above cited data might provide a clearer understanding of the impact of the material physical-biological properties on healing, graft stability and bone formation as suggested by Ebrahimi et al (2017) [2]. In this regard, bone is one of the few tissues that can fully repair itself by osteogenesis and healing process without any scar formation [24,25]. However, in some situations such as bone disease, extensive fracture or excision of bone

tumor, the loss of bone mass is too large to be self-repaired. The treatment of these cases is still controversial and there is a need for evidence-based treatment decision making, especially for those defined as critical sized defects. In general, despite variations on the defect dimensions between humans and animal models, a critical-sized defect is regarded as a wound that cannot heal spontaneously, requiring extra assistance to regenerate[15]. To achieve bone regeneration, new surgical techniques and novel tools could be used to obtaining favorable biological responses. In all cases, bone substitutes are necessary[16] and developing bone grafting materials with high ability to stimulating bone regeneration is an important strategy to achieve optimal bone repair. Preclinical models using rat[17] and rabbit[18]calvaria have been widely used. However, previous studies[17,18] suggest the necessity of a further standardization of critical size bone defect (CSBD) models to enable more accurate comparisons among studies considering: age, defect size, anatomical location, surgical technique to create the defect, evaluation method, period and following the 3Rs principles in animal testing[17].

Thus, the present study sought to perform the physicochemical characterization of a novel porous BCP and to evaluate *in vivo* its effectiveness in the repair of bone critical sized defects using three different sized pBCP granules embedded into blood clot versus use of autogenous bone (positive control) and blood clot (negative control). We hypothesized that granular size of BCPs has a direct influence on the healing response of the host tissues and on osteopromotion. Still there is a lack of knowledge and consensus regarding the role of granular size in bone regeneration.

MATERIALS AND METHODS

pBCP material

The pBCP developed by Baumer AS (Mogi Mirim, São Paulo, Brazil) was obtained using a chemical reaction between calcium hydroxide ($Ca(OH)_2$) and phosphoric acid (H_3PO_4) in a homogenous phase distribution. Varying the initial concentration of the starting materials and the conditions of pH and temperature under which the reaction took place, the hydroxyapatite/β-TCP ratio was reached. The exact HA/TCP ratio and crystallinity were documented by X-ray diffraction analysis. The macro porosity of the material was achieved by precipitating the BCP material on a polyurethane sponge. This impregnated sponge was heated in stages and sintered at a temperature above 900ºC to burn up the polymer material. The resulting porous blocks were crushed and sieved separating the granules by size. The resulting porous blocks were crushed and sieved separating the granules by size in pBCP1.5 (granules of 20–40 mesh with largest diameter up to 1.5 mm); pBCP1.0 (granules of 40–60 mesh, with largest diameter of 1.0 mm); and pBCP0.7 (granules of 60–80 mesh, which had an average of 0.7 mm at the largest diameter).

Physico-chemical characterization of pBCP

X-ray diffraction (XRD) and structural Rietveld Refinement: The crystal structure of powdered pBCPs samples was evaluated by XRD in A Rigaku, D/MAX 2100 PC diffractometer, using Cu-Kα radiation, 40 kV voltage, 20 mA current, divergence slit of 1 degree, receiving slit of 0.3 mm, nickel filter, through a 10 to 80º range of angular scan, step of 0.02º and fixed time of 1,6 s/step. For crystal structure indexing, theoretical cards PDF 72-1243 and 70-2065 related to hydroxyapatite hexagonal phase and *whitlockite* trigonal β-TCP

phase were used, respectively. Quantitative information regarding phase composition and lattice parameters were obtained from Structural Rietveld Refinement using the software GSAS and EXPGUI interface (TOBY, 2001; LARSON, 2004) and the Inorganic Crystal Structure Database cards ICSD 26-204 and ICSD 6-191 for HA and β-TCP, respectively.

Scanning electron microscopy (SEM) and Energy-dispersive X-ray spectroscopy (EDS): pBCPs were also dimensionally and morphologically characterized by SEM, using a Carl Zeiss EVO LS15 microscope (3 nm of theoretical resolution) equipped with a thermionic tungsten gun, operating at 15 kV. Before SEM characterization, samples were fixed over a double-face carbon tape placed over the stub and gold coated in order to confer conductor character to the samples, enabling electron microscopy analysis. Low magnification images were taken for the average grain size determination (20-25 particles for each sample and diagonal measurements). Using these data, both diagonals (D and d) average sizes as well as their respective standard deviations (SD) were calculated. Furthermore, high magnification images were taken disclosing further surface details. Elemental and chemical analysis of each pBCP sample was made using EDS Oxford INCA X-ACT integrated to SEM.

In vivo study

Animal and experimental groups: The experimental protocol followed "The Guiding Principles for the Care and Use of Animals", according to the principles of the Declaration of Helsinki, and was approved by the Institutional Review Board for Animal Research of Bauru School of Dentistry – University of São Paulo (Process n. CEEPA0 008/2005 and 13/2009). Seventy-five male Wistar rats aging 5 months and weighing 450-500 g, were used (Bauru School of Dentistry Animal Care Department). The rats were maintained in plastic cages in a

room with temperature between 22°C and 24°C, 12-hour light/dark controlled cycle and free access to food and water. The animals (n=75) were randomly divided into three treatment groups: 1) pBCP group (n=45) subdivided in three subgroups according to the mean size of the granules pBCP0.7, pBCP1.0 and pBCP1.5; AB group or positive control (n=15) and CSBD group or negative control (n=15) (see Figure 1A).

Surgical procedure: The animal surgeries were performed under general anesthesia with an intramuscular injection of 80 mg/Kg ketamine hydrochloride – Dopalen™ and 8mg/Kg of xylazine hydrochloride - Anasedan ™ (both of AgriBrands Purina do Brasil Ltda, Paulínia – SP, Brazil) with anesthesia state duration of approximately 25 min. The state of the anesthesia was monitored closely throughout the procedure and, when necessary, a 1/3 supplementation of the ketamine initial dose was performed. Under anesthesia a fronto-parietal trichotomy and **disinfection** with 10% povidone-**iodine** (PI) was performed. Then a half-moon incision was made on the skull skin and a total thigh musculocutaneous flap was raised posteriorly, exposing the cranial surface. Using an 8-mm diameter trephine bur with continuous irrigation, a full-thickness defect (Fig. 1A1) was created in the parietal bones of each rat, exposing the dura-mater in its bottom (Fig. 1A2). The cranial bone plug removed (Fig. 1A2) was fixed in 10% phosphate-buffered formalin for 48 hours for histological processing. In the pBCPs groups, the defects were filled with 80 mm^3 of pBCP particles homogenized with blood obtained by cardiac puncture (Fig. 1B1), AB group was filled with 80 mm^3 of particulate AB bone obtained from the calvarial plug (Figure 1B2) and CSD-control group solely with 80 mm^3 of blood clot (Fig. 1B3).

The post-operative care consisted of a subcutaneous injection of non-steroidal anti-inflammatory and analgesic flunixin meglumine (2.5 mg/Kg; Banamine*-Schering-Plough SA, Rio de Janeiro, Brazil) at 12 and 24 hours.

Samples collection and histological procedures: The animals of each group were sacrificed with an overdose of the ketamine/xylazine mixture (three times the anesthetic dose). The cranial vault bones with the lining skin were collected and fixed in 10% phosphate-buffered formalin for 48 hours. The specimens were demineralized in ethylenediamine tetraacetic acid (EDTA), a solution containing 4.13% Tritriplex III (Merck KGaA, Darmstadt, Germany) and 0.44% sodium hydroxide, for a period of approximately 40 days. Subsequently the pieces were submitted to histological processing for inclusion in polymer-enriched paraffin Histosec^{TM} (Merck KGaA, Darmstadt, Germany) and 5-µm thick coronal sections were obtained and stained with hematoxylin and eosin (HE).

Morphometric evaluations: Five coronal cross-section of each defect obtained approximately at 1 mm (S1), 2.5 mm (S2), 4.5 mm (S3), 5.5 mm (S4) and 6.5 mm (S5) of the anterior border towards the posterior border (Fig. 2A) were selected. For each section, a high-resolution image of the defect was obtained using a digital camera MC200 and a transmitted light microscope with x4 objective lens (Axioskop^{TM} Carl Zeiss MicroImaging GmbH, Jena, Germany) and subsequently with all images of each defect, its volume was reconstructed (Fig. 2B). The total volume (TV in mm^3) of the initial defect (bone plug removed) and of the grafted region in AB and pBCP groups was calculated using the formula for cylinder volume: $TV = [\pi . (D/2)^2 . h]$ where, "D" is the major diameter of defect and "h" is the average of vertical thicknesses of the grafted region as suggested by Cestari et al. (2009) [19] (see details in

the Fig. 2C).

The volume density (Vvi, %) of each structure or component present in the grafting area of pBCP and AB grafts and in defects of the CSBD group were determined manually using an image analysis system (AxioVision, Carl Zeiss, Germany). Firstly, the total area (TA) of grafted region in AB and pBCP groups (Fig. 2D3) and bone plug removed in CSBD group (Fig. 2D4) was determined. Next, the total area of each structure/component (TAi) was calculated surrounding manually the contour of each structure. The volume density (Vvi) of new bone, material/graft and connective tissue were calculated by the formula: Vvi = (TAi x 100)/TA (%). Then, the total volume of each structure (VTi) in the grafted region or defect was calculated by the following formula: VTi = (TV x Vvi)/100 (mm^3).

Statistical analysis

All statistical analyses were made with Prism 5.00 software for Windows (GraphPad Software, Inc., California, USA). First, all data obtained from total volume of defect/grafted area, and volume of graft material, newly formed bone and connective tissue were submitted to normality test (Kolmorov-Smirnov). Since this parameter was satisfied, the data were compared among periods and experimental groups by one-way analysis of variance (ANOVA), and the means contrasted by Tukey´s test. For all tests, $p<0.05$ was considered as the significance level.

RESULTS

Physico-chemical characterization

Crystal structure evaluation by X-ray diffraction (XRD), Rietveld structural refinement's plots and related results (Fig. 3) showed a similar diffraction pattern for all three pBCP powdered samples and it was possible to identify two different crystal structures (Figs. 3A1-A3): a hexagonal phase with the chemical formula [$Ca_{10}(PO_4)_6OH_2$] of the HA (PDF card number 72-1243) and a trigonal *whitlockite* phase with the chemical formula [$(Ca,Mg)_9(PO_4)_6$] of the b-TCP (PDF card number 70-2065).

Structural Rietveld refinements (Figs 3B1-B3) showed good compatibility between the theoretical and experimental patterns. The χ^2 values of 1.318 for pBCP0.7, 1.431 for pBCP1.0 and 1.479 for pBCP1.5 confirm that refinements went satisfactorily. According to the performed structural refinements (Figs. 3C1-C3) in all tested biomaterials, the proportion between HA and β-TCP was close to the values provided by the manufacturer (70/30). Lattice parameters for hexagonal hydroxyapatite and determined from Rietveld refinements were very similar to the theoretical ones (a = b = 9.432 Å and c = 6.881 Å). However, significant distortions were observed in all three lattice parameters for trigonal *whitlockite* β-TCP (a = b = 10.439 Å and c = 37.375 Å).

Dimensional, morphological and chemical evaluations of the pBCPs by scanning electron microscopy (SEM) and energy-dispersive X-ray spectrometry are shown in Figure 4.

The panoramic view and detailed view SEM images of pBCP0.7, pBCP1.0 and pBCP1.5 represented in Figure 4A showed a similar surface morphology with small concavities and microporosities. Larger (D) and smaller (d) diagonal average sizes were determined by SEM (Fig. 4D) and the values are shown in Table (Fig. 4E) where it is possible

to notice that, at least in one direction, the granule's average dimension is in agreement with the values provided by the manufacturer.

Qualitative and quantitative chemical composition analyzes were also performed by EDS and the results are shown in Figures 4B and 4C, respectively. According to EDS spectra for pBCP0.7, pBCP1.0 and pBCP1.5 (Fig. 4B) all HA and β-TCP constitutive elements were identified, i.e., calcium (Ca), phosphorous (P) and oxygen (O). Small peaks of magnesium (Mg) also observed in all analyzed samples are probably due to substitution of the magnesium atoms found in the trigonal *whitlockite* β-TCP. Furthermore, the observed gold (Au) peaks represent the conductive gold layer deposited over the particles for SEM analyzes. Lastly, in Figure 4C it is possible to notice a very similar quantitative chemical composition for all three tested pBCP, except for pBCP0.7 that presented a higher amount of calcium.

In vivo critical-size bone repair

Morphological and volumetric changes of grafted region and materials

Panoramic photomicrographs of the bone plug and bone defects of CSBD, AB, and pBCPs groups are presented in Figure 5, together with the graphics of the total volume (TV) of the bone plug and grafted region and volume of materials (MV).

The 8mm critical-size bone defect in the rat calvaria included two parietal bones and the sagittal suture. The bone plug (Fig. A1 and A2) represents the parietal bone removed surgically or the bone lost. The parietal bones are constituted by two bony cortices and between them small and few medullary cavities. The TV of the bone plug removed of all defects was similar among groups, being on average of 31.3 ± 2.25 mm^3 (p=0.3694). In CSBD group, no closure of the defects occurred and small bone formation was restricted to their edges (see Figs. A2 and B2). In AB defects, the bone formation was present in all

grafted area connecting the AB particles (A3 and B3), while in pBCP defects the osteogenesis occurred initially at the defect border and near to dura mater surface going towards the center of the defect and tegument region. In the defects filled with AB and pBCPs the grafted volume was 2.82 times higher than the bone plug at 4 weeks being on average of 88.5 ± 6.65 mm^3 (see Figs. A3-A6 and graph C). Although no differences were observed between TV of AB and pBCPs groups at 4 weeks, a significant and gradual reduction of 45% in the grafted volume was observed only in AB group until 24 weeks (compare Fig. A3 and B3). This reduction of the grafted volume was accompanied by a reduction of 37% of the TV of AB particles. On the other hand, the MV of pBCP granules of different sizes maintained constant during all experimental periods, being in average of 38.2 ± 6.31 mm^3 (p=0.9367).

Histological and volumetric differences of bone formation in the defects treated with AB and pBCP with different granule size

The histological details of bone repair in the critical-size defects treated with AB and pBCP with different granule size, and graphics of the total volume of bone (BV) and soft tissue (STV) morphometrically evaluated are presented in Figure 6.

At 4 weeks, AB treated defects showed major bone formation (BV = 32.6 ± 6.38 mm^3) filling 61.1% of the spaces between particles (see Fig. A1 and Graph 6E). In the same period, pBCP treated defects (Figs B1, C1 and D1) presented initially bone formation in the spaces between the granules located near to duramater while the intergranular spaces near to tegument was filled by connective tissue. In pBCP groups, only 24.4% of the spaces between granules were filled by newly formed bone (BV=12.3 ± 3.8 mm^3) and 75.6% by connective tissue (CTV=38 ± 4.61 mm^3) (see graphics 6E and 6D). Between 4 and 24 weeks, a large reduction of the total volume of the grafted region (compare Fig. A1 with A3) occurred in AB due to a decrease of 37% on AB particles volume (graph of Fig. 5D) and only 44.6% of newly

formed bone (graph of Fig. 6E). Contrasting with this, a significant increase of bone formation between 4 and 24 weeks happened in all pBCP groups, reaching the spaces between the granules located near the tegumental region. At 24 weeks, the volume of newly formed bone was higher in pBCP1.0 (BV = 38 ± 5.1mm^3), followed by pBCP0.7 (BV = 31.3 ± 6.24 mm^3), pBCP1.5 (BV=22.6 ± 5.28 mm^3) and AB (BV=18.5 ± 4.7mm^3) (see graphic 6E).

DISCUSSION

In the present work, our result showed that the novel pBCP containing hydroxyapatite and β-TCP with 70/30 ratio embedded into a blood clot can promote a large new bone formation in the critical-size bone defect in rat skull when compared to AB. However, the quantity of bone formation is dependent of the granular size.

Clinically, most of bone substitutes used have granules between 0.1 and 5 mm in diameter, and they are frequently mixed with the patient's aspirated blood. In the current work, we emphasize the importance of the blood clot in the agglutination of pBCP granules that facilitates their implantation and stability in the defect site. Besides, the fibrin scaffold connecting the pBCP granules and the blood proteins adsorbed on theirs surfaces favor angiogenesis, migration, proliferation and attachment of osteoblasts facilitating bone tissue repair. The pBCP capacity to adsorb biological fluids, including the entrapment of proteins and other molecules was related mostly to the microporosities present in its surface [20]. Considering that the pBCP scaffolds analyzed here were rich in micropores, this may have contributed to adsorption of blood proteins, thus favoring bone repair. The effect of porous structures on protein adsorption has been considered as an interpretation of the osteoinductive potential of Ca-P bioceramics after implantation in ectopic sites observed in the pBCP70:30[10] and other BCPs[21,22]. It is worth pointing out that the hematoma/blood clot produced

immediately following a bone injury is considered a vital element for bone healing. Removal of the initial fracture hematoma impairs the repair process, whereas implantation of a hematoma can yield new bone formation in rodents [23] and bovines[24]. More recently, it was observed that whole blood clotted around BCP microparticles was able to induce ectopic bone formation after subcutaneous implantation in C57BL/6 mice as well as to repair critical-sized femoral defects in rats[25,26] and that the mononuclear cell fraction present in the blood was involved in the new bone formation.

The bone volume of the plug removed surgically using an 8-mm trephine bur was in mean of 31.3±2.25 mm^3. In CSBD defects, no closure of the defect was observed until 24 weeks and the volume of formed bone was only 30% of bone plug (BV = 9.57±4.67 mm^3), highlighting the importance of the use of bone graft substitutes. AB graft, due to the combination of osteoinductive, osteoconductive and osteogenic properties [27] promoted bone formation in all grafted area connecting the AB particles, while in defects filled with pBCP osteogenesis occurred from the border of the defects and dura mater proximity toward the center of the defect and to integumentary region which highlights a high osteoconductive characteristic [28]. At 4 weeks, AB treatment demonstrated to be superior to pBCP, promoting higher bone gain (32.6±6.4 mm^3), which is similar to the bone plug removed, while for the pBCPs the bone gain was only of 36% (12.27 ± 3.79 mm^3), similar to that of CSBD defects.

However, in AB defects the initial bone formation and graft were not maintained until 24 weeks. Between 4 and 24 weeks, a higher reduction of 44.63% in the bone gain (32.6 mm^3 at 4 weeks to 18.05 mm^3 at 24 weeks) and 37% of AB particles (27.69 mm^3 at 4 weeks to 17.44 mm^3 at 24 weeks) led to reduction of 24.14% in the grafted volume and increase of bone marrow space. On this issue, AB showed higher rate of particle graft remodeling and reduction. Only 4.8% of AB particles were found after 24 weeks of healing in the maxillary sinus augmentation procedure[29]. In a different manner, in all pBCP treatments the grafted

volume was stable during all experimental periods (mean of 90.17± 6.58 mm^3), due to small absorption of pBCP granules (means of 40.61±4.0 mm^3 at 4 weeks and 37.13±4.15mm^3 at 24 weeks). A reason for the small degradation of the pBCP was the higher percentage of the more stable (HA, 70%) than the more soluble (β-TCP, 30%) phases, as confirmed by XRD and structural Rietveld Refinements. In addition, the higher ionic dissolution of β-TCP results in microcrystals formation in a supersaturated microenvironment [1,30] that leads to an increase of multinucleated cells on the pBCP surfaces [31]. Thus, a greater ratio of HA decreased osteoclasts activity to reabsorb the BCP [5]. The stable pBCP 70:30 can help to preserve the bone that was formed in the early healing phases and maintain a microenvironment between granules auspicious for bone growth. This suggests that the novel pBCP can be applied to large bone defects that will maintain their shape over long periods of time [32,33]. Comparatively, Jensen et al. (2008) also observed a decrease in the amount of initial bone formation in the mandibular defects grafted with materials of high degradation rates (coagulum, autograft, and BCP 20/80) versus less degradable oness (BCP 80/20, BCP 60/40 and DBBM) that were still observed after 52 weeks. On the other hand, in the rabbit maxillary sinus augmentation, the volume stability and osteoconductive capacity of BCP with an HA/β-TCP ratio of 30:70 was comparable to that of HA/β-TCP ratio of 70:30 in a short period of healing (2 and 8 weeks), but a significant more resorption of BCP 30:70 than BCP 70:30 was observed [34].

The BCP physical structure, frequency, size and shape of pores, play an important role in several stages of new bone formation, such as cell adhesion and tissue ingrowth [20,35]. Although porosity was not quantified in the present study, the materials studied here contained concavities and pore structures at both, the micro- and macroscale, leading to increase in its specific surface area. Histologically, the presence of concavities in pBCP created a favorable microenvironment which directly modulated cell responses for bone

formation. The presence of blood clot with high level of calcium and phosphate ions results of the BCP dissolution, promotes cell colonization, differentiation, adhesion and bone formation (see Fig. 7). It is worth mentioning that all pBCP used in this study showed a similar crystallinity, chemical composition and surface morphology, varying only in the size of granules. In all defects filled with different granule sizes, pBCP0.7, pBCP1.0 and pBCP1.5, the grafted volume was in average 188% higher than bone plug (90.17 mm^3 vs. 31.3 mm^3). The residual materials occupied in average 43.65% of the defect during all experimental periods and the bone formation was gradually occupied the space between the particles (56.35% of defect). Although at 4 weeks no difference was observed regarding bone formation of all pBCP groups (average of 12.27 mm^3), a higher bone increase was observed in pBCP1.0 (183.5%, BV=38.05 mm3) followed by pBCP0.7 (166.32, BV=31.33 mm^3) and pBCP1.5 (94.06%, BV=22.57 mm^3) until 24 weeks. The BV of pBCP1.0 and pBCP 0.7 did not show changes, but in pBCP 1.5 it was 40.12% smaller compared to pBCP1.0. Differences in cell response have also been shown in the *in vitro* approach on granular BCPs with HA/β-TCP ratio (65/35) of diverse granule sizes and porous blocks. The hMSCs proliferated to a greater extent over the small granules (BCP0.7) while large granules (BCP1.5) and blocks promoted quicker hMSCs differentiation [8], highlighting the importance of the granule size. In respect to other grafting materials, Pallesen and colleagues (2002) [13] reported an inverse relationship between particle size and volume of newly formed bone after using autografts in standardized calvarial defects of rabbits. On the other hand, a recent case series of 10 patients compared small (0.25-1mm) and large (1mm-2mm) deproteinized bovine bone matrix particles for sinus floor elevation and showed no difference regarding bone volume in biopsies harvested after 6 to 9 months of healing [36].

CONCLUSION

This is a first study that evaluated the physicochemical parameters of this pBCP HA/β-TCP 70:30, correlating them with its with biological behavior, using a standardized preclinical model for bone regeneration. We showed that the presence of concavities in pBCP surface create a favorable microenvironment for bone formation, which is directly influenced by the granule size. Future clinical studies should be conducted to evaluate the performance of these materials.

ACKNOWLEDGEMENTS

To Brazilian Funding Agencies for supporting this research: FAPESP (processes 05/02221-8 and 05/02310-0) and to Danielle Santi Ceolin, for her help with histotechnical processing. The sintered anorganic bone (Gen-Ox-Inorg^{TM}) was donated by Baumer S.A., Mogi Mirim – São Paulo, Brazil.

REFERENCES

1. LeGeros RZ, Lin S, Rohanizadeh R, Mijares D, LeGeros JP. Biphasic calcium phosphate bioceramics: preparation, properties and applications. Journal of Materials Science: Materials in Medicine 2003;14(3):201-209.

2. Ebrahimi M, Botelho MG, Dorozhkin SV. Biphasic calcium phosphates bioceramics (HA/TCP): Concept, physicochemical properties and the impact of standardization of study protocols in biomaterials research. Mater Sci Eng C Mater Biol Appl 2017;71:1293-1312.

3. Nery EB, LeGeros RZ, Lynch KL, Lee K. Tissue response to biphasic calcium phosphate ceramic with different ratios of HA/beta TCP in periodontal osseous defects. J Periodontol 1992;63(9):729-35.

4. Park JW, Kim ES, Jang JH, Suh JY, Park KB, Hanawa T. Healing of rabbit calvarial bone defects using biphasic calcium phosphate ceramics made of submicron-sized grains with a hierarchical pore structure. Clin Oral Implants Res 2010;21(3):268-76.

5. Farina NM, Guzon FM, Pena ML, Cantalapiedra AG. In vivo behaviour of two different biphasic ceramic implanted in mandibular bone of dogs. J Mater Sci Mater Med 2008;19(4):1565-73.

6. Yun PY, Kim YK, Jeong KI, Park JC, Choi YJ. Influence of bone morphogenetic protein and proportion of hydroxyapatite on new bone formation in biphasic calcium phosphate graft: two pilot studies in animal bony defect model. J Craniomaxillofac Surg 2014;42(8):1909-17.

7. Yang C, Unursaikhan O, Lee JS, Jung UW, Kim CS, Choi SH. Osteoconductivity and biodegradation of synthetic bone substitutes with different tricalcium phosphate contents in rabbits. J Biomed Mater Res B Appl Biomater 2014;102(1):80-8.

8. Lobo SE, Glickman R, da Silva WN, Arinzeh TL, Kerkis I. Response of stem cells from different origins to biphasic calcium phosphate bioceramics. Cell Tissue Res 2015;361(2):477-95.

9. Wang L, Barbieri D, Zhou H, de Bruijn JD, Bao C, Yuan H. Effect of particle size on osteoinductive potential of microstructured biphasic calcium phosphate ceramic. J Biomed Mater Res A 2015;103(6):1919-29.

10. Santos PS, Cestari TM, Paulin JB, Martins R, Rocha CA, Arantes RVN, Costa BC, Dos Santos CM, Assis GF, Taga R. Osteoinductive porous biphasic calcium phosphate ceramic as an alternative to autogenous bone grafting in the treatment of mandibular bone critical-size defects. J Biomed Mater Res B Appl Biomater 2018;106(4):1546-1557.

11. Albert DE. 5 - Material and chemical characterization for the biological evaluation of medical device biocompatibility. In: Boutrand J-P, editor. Biocompatibility and Performance of Medical Devices: Woodhead Publishing; 2012. p 65-94.

12. Ebrahimi M, Pripatnanont P, Monmaturapoj N, Suttapreyasri S. Fabrication and characterization of novel nano hydroxyapatite/beta-tricalcium phosphate scaffolds in three different composition ratios. J Biomed Mater Res A 2012;100(9):2260-8.

13. Pallesen L, Schou S, Aaboe M, Hjorting-Hansen E, Nattestad A, Melsen F. Influence of particle size of autogenous bone grafts on the early stages of bone regeneration: a histologic and stereologic study in rabbit calvarium. Int J Oral Maxillofac Implants 2002;17(4):498-506.

14. Barbeck M, Dard M, Kokkinopoulou M, Markl J, Booms P, Sader RA, Kirkpatrick CJ, Ghanaati S. Small-sized granules of biphasic bone substitutes support fast implant bed vascularization. Biomatter 2015;5(1):e1056943-e1056943.

15. Cameron JA, Milner DJ, Lee JS, Cheng J, Fang NX, Jasiuk IM. Employing the biology of successful fracture repair to heal critical size bone defects. Curr Top Microbiol Immunol 2013;367:113-32.

16. Yuan H, Barbieri D, Luo X, Van Blitterswijk CA, de Bruijn J. Calcium Phosphates and Bone Induction; 2017.

17. Vajgel A, Mardas N, Farias BC, Petrie A, Cimoes R, Donos N. A systematic review on the critical size defect model. Clin Oral Implants Res 2014;25(8):879-93.

18. Delgado-Ruiz RA, Calvo-Guirado JL, Romanos GE. Critical size defects for bone regeneration experiments in rabbit calvariae: systematic review and quality evaluation using ARRIVE guidelines. Clin Oral Implants Res 2015;26(8):915-930.

19. Cestari TM, Granjeiro JM, de Assis GF, Garlet GP, Taga R. Bone repair and augmentation using block of sintered bovine-derived anorganic bone graft in cranial bone defect model. Clin Oral Implants Res 2009;20(4):340-50.

20. Cheng L, Ye F, Yang R, Lu X, Shi Y, Li L, Fan H, Bu H. Osteoinduction of hydroxyapatite/beta-tricalcium phosphate bioceramics in mice with a fractured fibula. Acta Biomater 2010;6(4):1569-74.

21. Yuan H, Fernandes H, Habibovic P, de Boer J, Barradas AMC, de Ruiter A, Walsh WR, van Blitterswijk CA, de Bruijn JD. Osteoinductive ceramics as a synthetic alternative to autologous bone grafting. Proceedings of the National Academy of Sciences 2010;107(31):13614.

22. Yuan H, Kurashina K, de Bruijn JD, Li Y, de Groot K, Zhang X. A preliminary study on osteoinduction of two kinds of calcium phosphate ceramics. Biomaterials 1999;20(19):1799-806.

23. Grundnes O, Reikeras O. The importance of the hematoma for fracture healing in rats. Acta Orthop Scand 1993;64(3):340-2.

24. Schell H, Duda GN, Peters A, Tsitsilonis S, Johnson KA, Schmidt-Bleek K. The haematoma and its role in bone healing. Journal of experimental orthopaedics 2017;4(1):5-5.

25. Balaguer T, Boukhechba F, Clave A, Bouvet-Gerbettaz S, Trojani C, Michiels JF, Laugier JP, Bouler JM, Carle GF, Scimeca JC and others. Biphasic calcium phosphate microparticles for bone formation: benefits of combination with blood clot. Tissue Eng Part A 2010;16(11):3495-505.

26. Paul AJ, Momier D, Boukhechba F, Michiels JF, Lagadec P, Rochet N. Effect of G-CSF on the osteoinductive property of a BCP/blood clot composite. J Biomed Mater Res A 2015;103(9):2830-8.

27. Galindo-Moreno P, Avila G, Fernandez-Barbero JE, Mesa F, O'Valle-Ravassa F, Wang HL. Clinical and histologic comparison of two different composite grafts for sinus augmentation: a pilot clinical trial. Clin Oral Implants Res 2008;19(8):755-9.

28. Bouler JM, Pilet P, Gauthier O, Verron E. Biphasic calcium phosphate ceramics for bone reconstruction: A review of biological response. Acta Biomater 2017;53:1-12.

29. Danesh-Sani SA, Wallace SS, Movahed A, El Chaar ES, Cho SC, Khouly I, Testori T. Maxillary Sinus Grafting With Biphasic Bone Ceramic or Autogenous Bone: Clinical, Histologic, and Histomorphometric Results From a Randomized Controlled Clinical Trial. Implant Dent 2016;25(5):588-93.

30. Daculsi G, Baroth S, LeGeros R. 20 years of Biphasic Calcium Phosphate Bioceramics Development and Applications; 2010. 45-58 p.

31. Bodde EW, Wolke JG, Kowalski RS, Jansen JA. Bone regeneration of porous beta-tricalcium phosphate (Conduit TCP) and of biphasic calcium phosphate ceramic (Biosel) in trabecular defects in sheep. J Biomed Mater Res A 2007;82(3):711-22.

32. Daculsi G, LeGeros RZ, Heughebaert M, Barbieux I. Formation of carbonate-apatite crystals after implantation of calcium phosphate ceramics. Calcif Tissue Int 1990;46(1):20-7.

33. Pripatnanont P, Prasertthem P, Suttapreyasri S, Leepong N, Monmaturapoj N. Bone Regeneration Potential of Biphasic Nanocalcium Phosphate with High Hydroxyapatite/Tricalcium Phosphate Ratios in Rabbit Calvarial Defects. Int J Oral Maxillofac Implants 2016;31(2):294-303.

34. Lim HC, Zhang ML, Lee JS, Jung UW, Choi SH. Effect of different hydroxyapatite:beta-tricalcium phosphate ratios on the osteoconductivity of biphasic calcium phosphate in the rabbit sinus model. Int J Oral Maxillofac Implants 2015;30(1):65-72.

35. Xia L, Lin K, Jiang X, Fang B, Xu Y, Liu J, Zeng D, Zhang M, Zhang X, Chang J and others. Effect of nano-structured bioceramic surface on osteogenic differentiation of adipose derived stem cells. Biomaterials 2014;35(30):8514-27.

36. Chackartchi T, Iezzi G, Goldstein M, Klinger A, Soskolne A, Piattelli A, Shapira L. Sinus floor augmentation using large (1-2 mm) or small (0.25-1 mm) bovine bone mineral particles: a prospective, intra-individual controlled clinical, micro-computerized tomography and histomorphometric study. Clin Oral Implants Res 2011;22(5):473-80.

Figure legends

Figure 1: *In vivo* study. A) Critical-size bone defect model: A1) Creation of the bone defect in parietal bone using a 8mm-trephine burr;and A2) bone plug (black arrow) completely removed from cut bony edge and full-thickness bone defect (blue arrow) exposing of the dura mater/brain (blue arrow).. B) Experimental groups and periods: B1) Defects filled with pBCP of different size, 0.7mm (n=15), 1.0mm (n=15) and 1.5mm (n=15); B2) defect filled particulate autogenous bone (AB, n=15) obtained from the bone plug removed (black arrow in A2); and B3) defect filled with blood clot (CSBD, n=15). At 2, 12 and 24 weeks five defects per group were evaluated.

Figure 2: Histomorfometric evaluations. A) Determination of total volume (mm^3) of grafted area and bone plug/bone lost: A1) defect filled with pBCP (A1a), AB (A1b) and CSBD (A1c) shows the proximate location of the five coronal 4µm-sections (S1, S2, S3, S4 and S5) evaluated; A2) central section of the defect (S3) showing the major diameter between defect borders (dotted line in red) and the heights of the grafted area (B1 and B2) and bone plug (B3) obtained at every 80µm of distance; and A3) cylindrical volume formula used for determination of the total volume of the grafted area and plug bone. B) Histological section of pBCP (B1) and AB (B2) and CSBD (B4) groups show the area evaluated (dotted blue area) for determination of volume density (%) of each structure/component.Note that in CSBD (B4) the area evaluated is referent to bone plug (B3).

Figure 3: Crystal structure characterization of pBCPs with different sizes by X-ray diffraction (DRX) and Rietveld structural refinement method: A1-A3) x-ray powder patterns show diffraction peaks of hydroxyapatite (HA, red asterisks) and tricalcium

phosphate (β-TCP, blue asterisks); B1-B3) Rietveld structural refinement's plots show good adjustment between experimental and theoretical standards; and C1-C3) table showing the HA and β-TCP proportions within the samples.

Figure 4: Morphological, dimensional and chemical features by SEM and EDS of the pBCPs with different sizes. A) SEM panoramic and detailed view of the pBCPs show similar morphology of the surfaces. See in details presence of many concavities on pBCP surface; B) X-ray energy spectrum of pBCPs show C, O, P, Ca, Mg and Au peaks; C) table containing mean and SD of each element and the Ca/P ratio obtained in the pBCPs samples; D) diagram showing dimensional measurements in both larger (D) and smaller diagonals (d) of the pBCP samples; and E) table containing the mean±SD of granule sizes of each pBCP samples. n=5 samples per pBCP granule size.

Figure 5: Panoramic histological view of the bone plug and bone defect at 4 (A1-A6) and 24 weeks (B1-B5), total volume of bone lost and grafted region (TV in C) and graft volume (MV in D) at all experimental periods. The bone plug is composed by a dense cortical bone containing rare marrow spaces and its volume was used as TV in CSBD group. At 4 weeks, the TV in the defects filled with AB and pBCPs (dotted blue line in A3-A6 and graph C) are similar among groups and higher than in CSBD. At 24 weeks the TV in pBCP groups (dotted blue line in B4-B6 and C) remained similar, while in AB (dotted blue line in B3 and C) it reduced significantly. The pBCP′s MV (black arrow in A3-A6 and B4-B6, graph D) remained constant along periods while in AB it reduced until 12 weeks. Bone formation (blue arrow) in CSBD (A2 and B2) is restricted to the defect borders while in AB it appeared in all grafted area merged with the AB particles (A3 and B3). In the pBCPs bone forms (blue arrow) initially from the borders of the defect then above the duramater, and toward the center

(compare A4-A6 with B4-B6). HE, 4X objective and scale bar =2mm. In the graphics bars=standard deviation and different letter are $p<0.05$ among groups and period by One-way ANOVA.

Figure 6: Histological images of the bone defect filled with AB and pBCPs, and graphs of new bone (NBV) and soft tissue (STV) volumes of the different groups at all experimental periods. In the defects filled with AB (A1-A3) all graft particles (black dot lined area) between the tegumentar (Te) and duramater (DM) regions are surrounded by newly formed bone (blue arrow) connecting the particles. In pBCP groups, from 4 (B1, C1 and D1) to 24 weeks (B3, C3 and D3), new bone formation (blue arrow) occurred proximate to the duramater (DM) growing toward tegument (Te). See the new bone level represented by blue dotted line. Graphically, the NBV (graphic E) in AB is higher than pBCPs at 4 weeks but it evolves inversely proportional until 24 weeks, however, pBCP0.7 and pBCP1.0 promoted higher bone formation than pBCP1.5 at 24 weeks. Between 4 to 24 weeks the STV (graphic F) reduce in all experimental groups except in CSBD group. HE, 10X objective and scalebar=2mm. In graphs bars=standard deviation and different letter are $p<0.05$ among groups and periods by One-way ANOVA.

Figure 7: Evolution of new bone formation into the concavities of pBCPs. A) SEM view of the pBCP surface shows numerous concavities (blue arrow); B-E) Temporal histological events shows in (B) pBCP concavities (blue arrows) initially filled by blood and soft connective tissue; (C) Concavities filled by soft connective tissue in the central region and fibrous connective tissue surrounding the pBCP surface; (D) Concavities filled by connective tissue in the central region and bone tissue surrounding its surface; and (E) Concavities fulfilled by bone. HE, 40X objective and scale bar=2mm

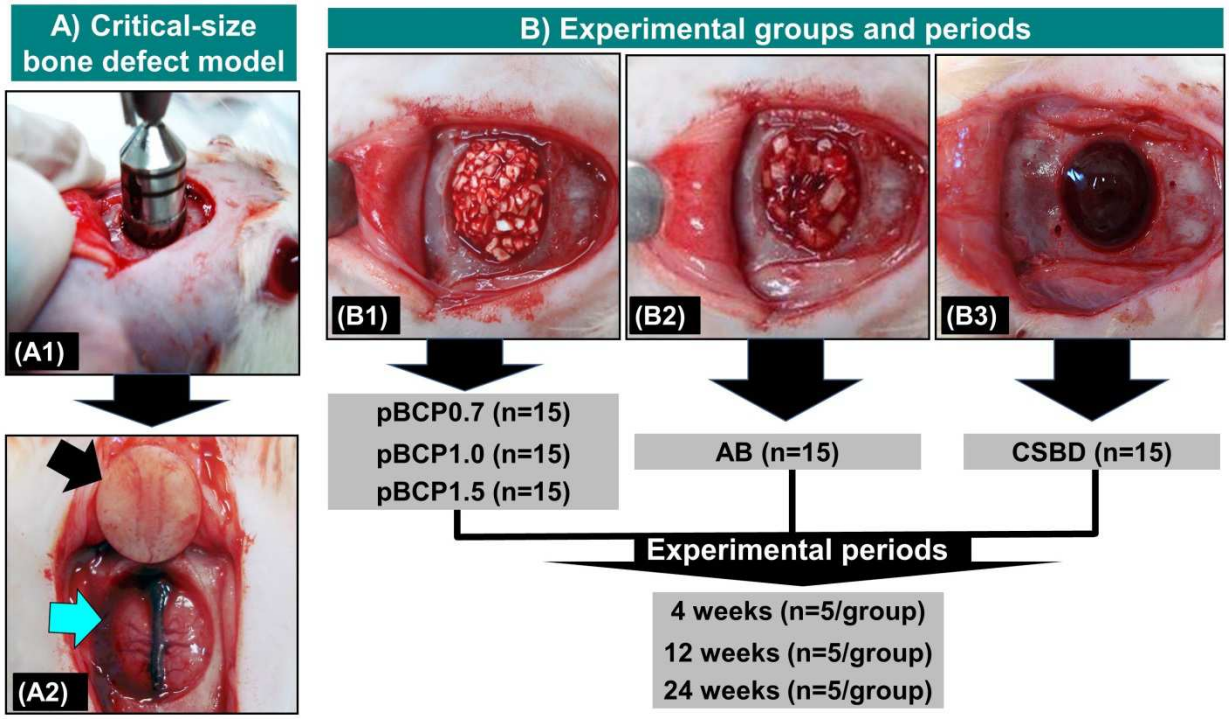
A) Critical-size bone defect model
(A1)
(A2)
B) Experimental groups and periods
(B1)
(B2)
(B3)
pBCP0.7 (n=15)
pBCP1.0 (n=15)
pBCP1.5 (n=15)
AB (n=15)
CSBD (n=15)
Experimental periods
4 weeks (n=5/group)
12 weeks (n=5/group)
24 weeks (n=5/group)

Figure 1

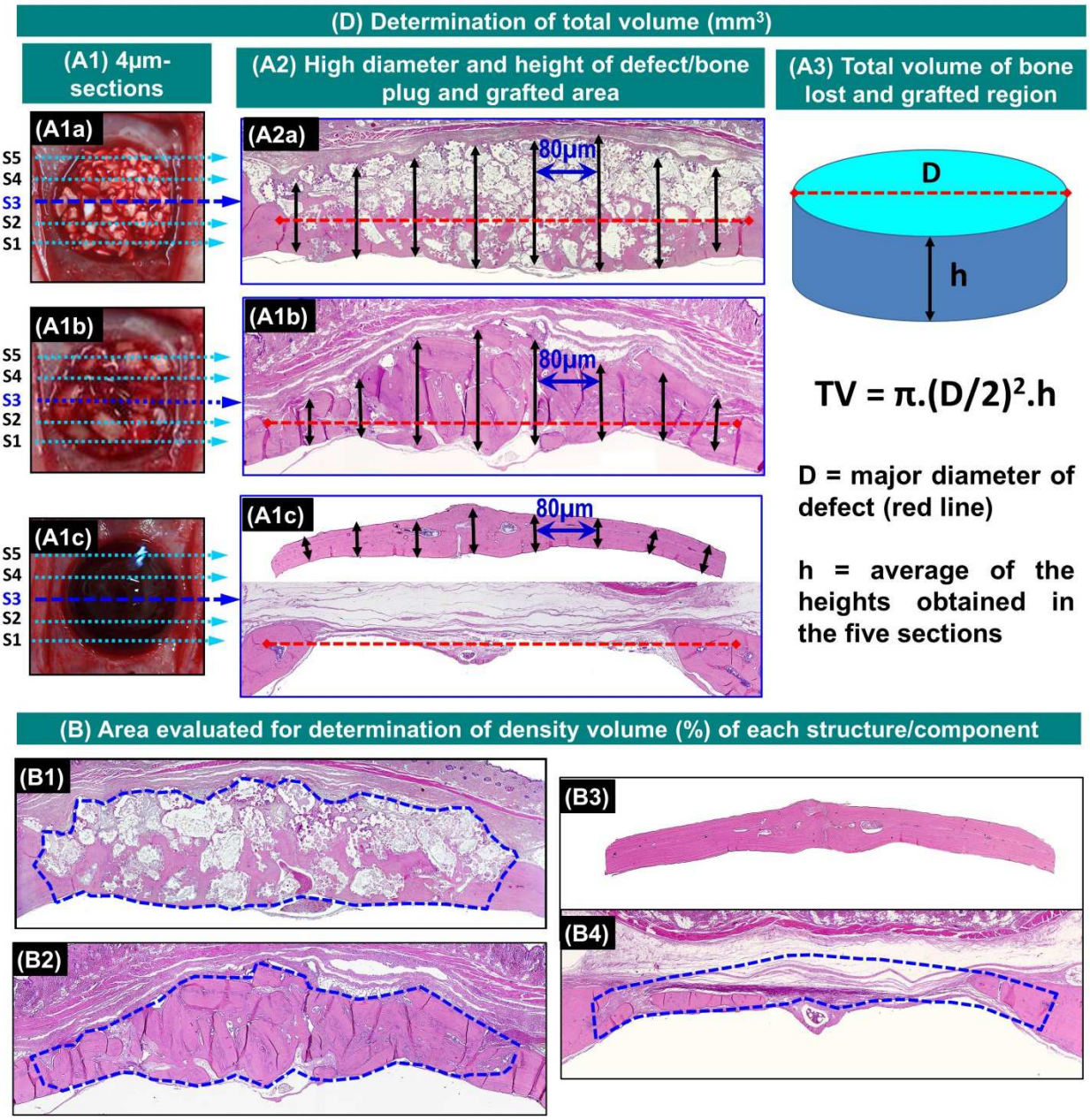
(D) Determination of total volume (mm³)
(A1) 4µm-sections
(A2) High diameter and height of defect/bone plug and grafted area
(A3) Total volume of bone lost and grafted region
(A1a)
(A1b)
(A1c)
S5
S4
S3
S2
S1
(A2a)
(A1b)
(A1c)
80µm
D
h
TV = π.(D/2)².h
D = major diameter of defect (red line)
h = average of the heights obtained in the five sections
(B) Area evaluated for determination of density volume (%) of each structure/component
(B1)
(B2)
(B3)
(B4)

Figure 2

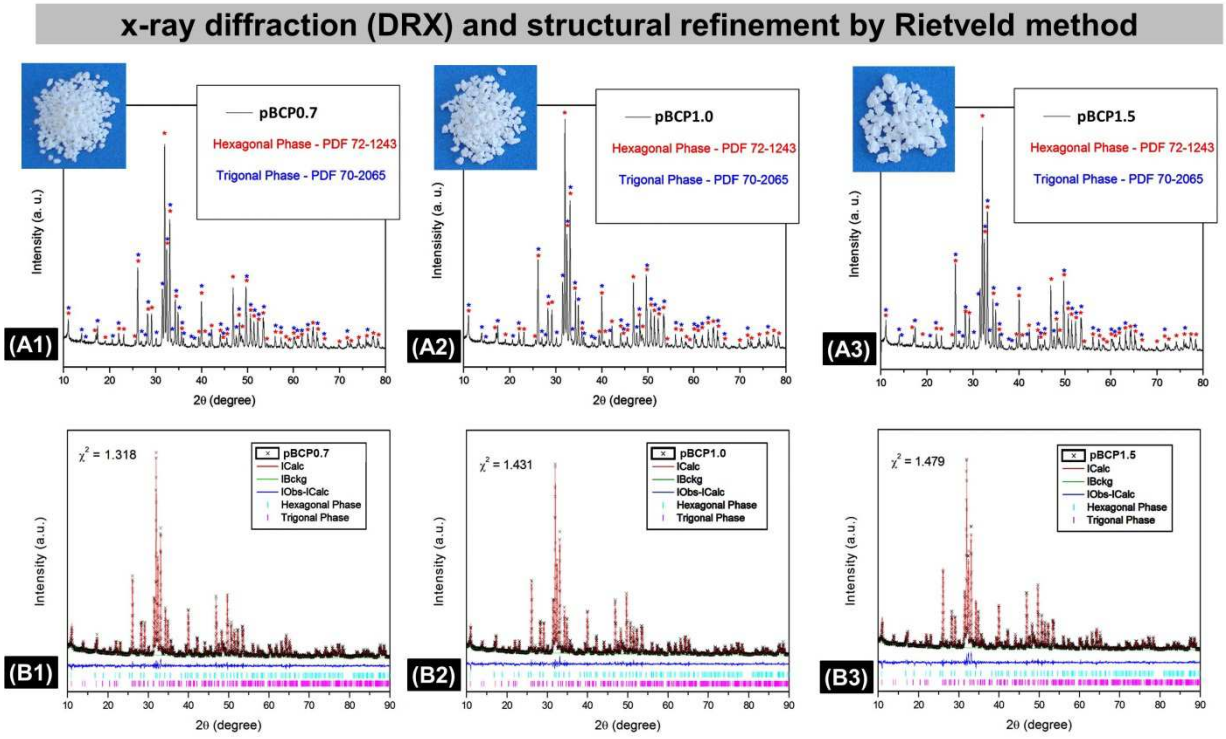

(C1) pPCB0.7 X^2 = 1.318

Lattice Parameter	Hexagonal Hydroxyapatite (HA)	Trigonal tricalcium phosphate (TCP)
a	9.429 Å	10.346 Å
b	9.429 Å	10.346 Å
c	6.878 Å	37.121 Å
% wt	71.81%	28.19%

(C2) pPCB1.0 X^2 = 1.431

Lattice Parameter	Hexagonal Hydroxyapatite (HA)	Trigonal tricalcium phosphate (TCP)
a	9.429 Å	10.345 Å
b	9.429 Å	10.345 Å
c	6.878 Å	37.115 Å
% wt	71.98%	28.02%

(C3) pPCB1.5 X^2 = 1.479

Lattice Parameter	Hexagonal Hydroxyapatite (HA)	Trigonal tricalcium phosphate (TCP)
a	9.428 Å	10.345 Å
b	9.428 Å	10.345 Å
c	6.878 Å	37.113 Å
% wt	71.27%	28.73%

Figure 3

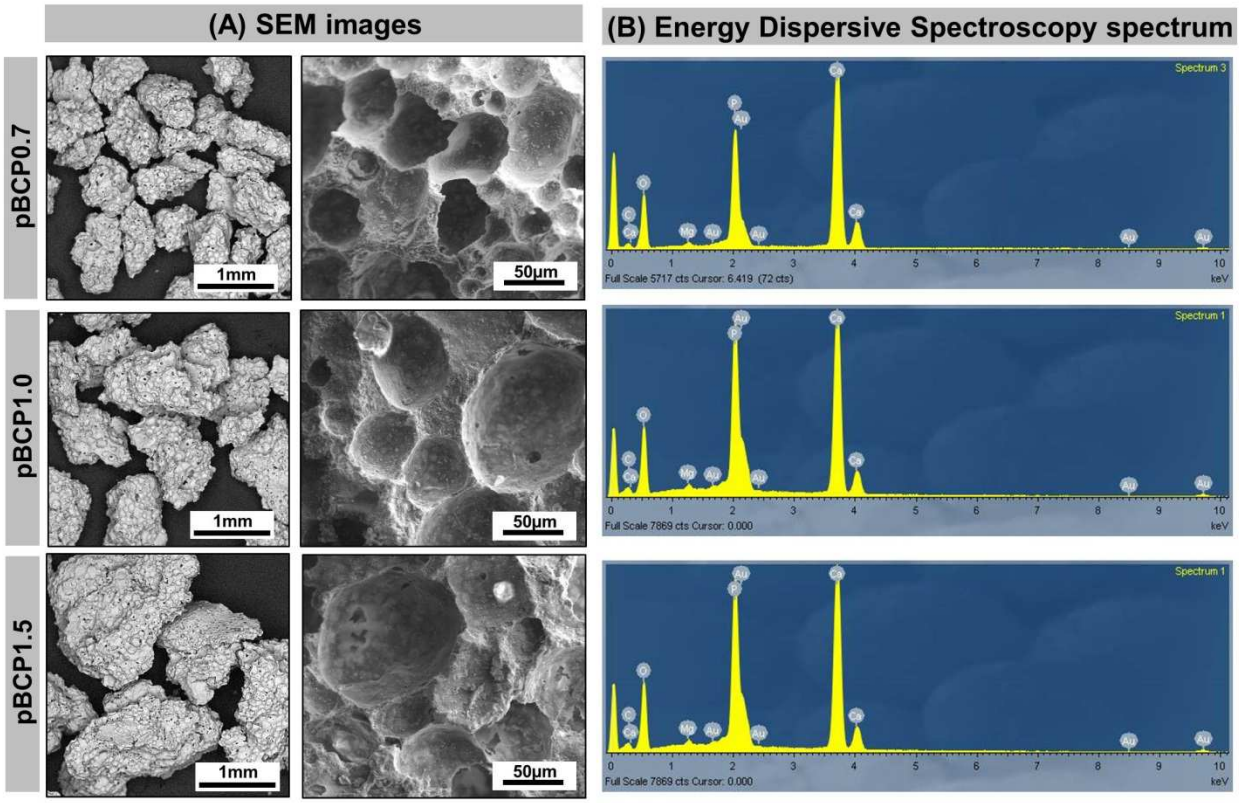

pBCP granule (size in mm)		(C) Surface chemical composition						Ca/P ratio
		C	O	Mg	P	Ca	Au	
pBCP0.7)	mean	6.42	55.24	0.37	11.43	25.44	1.32	2.22
	SD	± 2.95	±4,29	±0,06	±0,68	±5,75	±0,31	
pBCP1.0	mean	7,28	54,99	0,39	13,29	21,98	1,37	1.65
	SD	±0,36	±2,22	±0,04	±1,10	±1,20	±0,18	
pBCP1.5	mean	7,96	58,08	0,39	12,50	19,67	1,49	1.57
	SD	±1,07	±1,14	±0,06	±0,67	±1,38	±0,06	

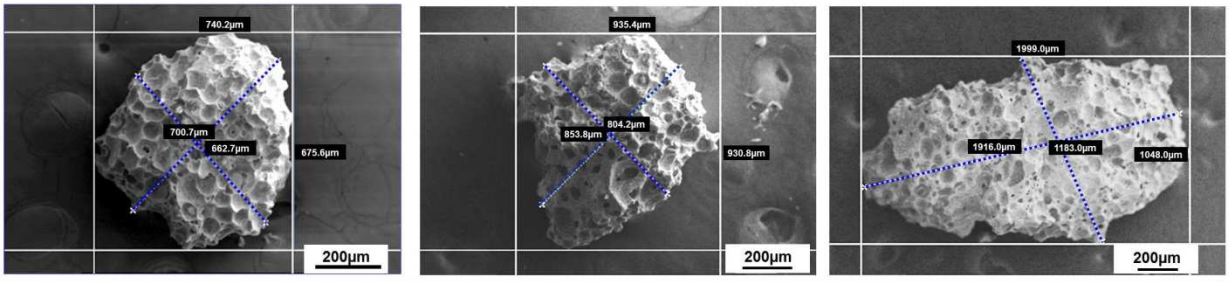

(E) Granule diameter (Mean ± SD)					
pBCP0.7		pBCP1.0		pBCP1.5	
D (µm)	d (µm)	D (µm)	d (µm)	D (µm)	d (µm)
892.5 ± 120.3	613.5 ± 88.5	1151.0 ± 228.9	828.0 ± 93.1	1721.5 ± 228.7	1285.5 ± 178.7

Figure 4

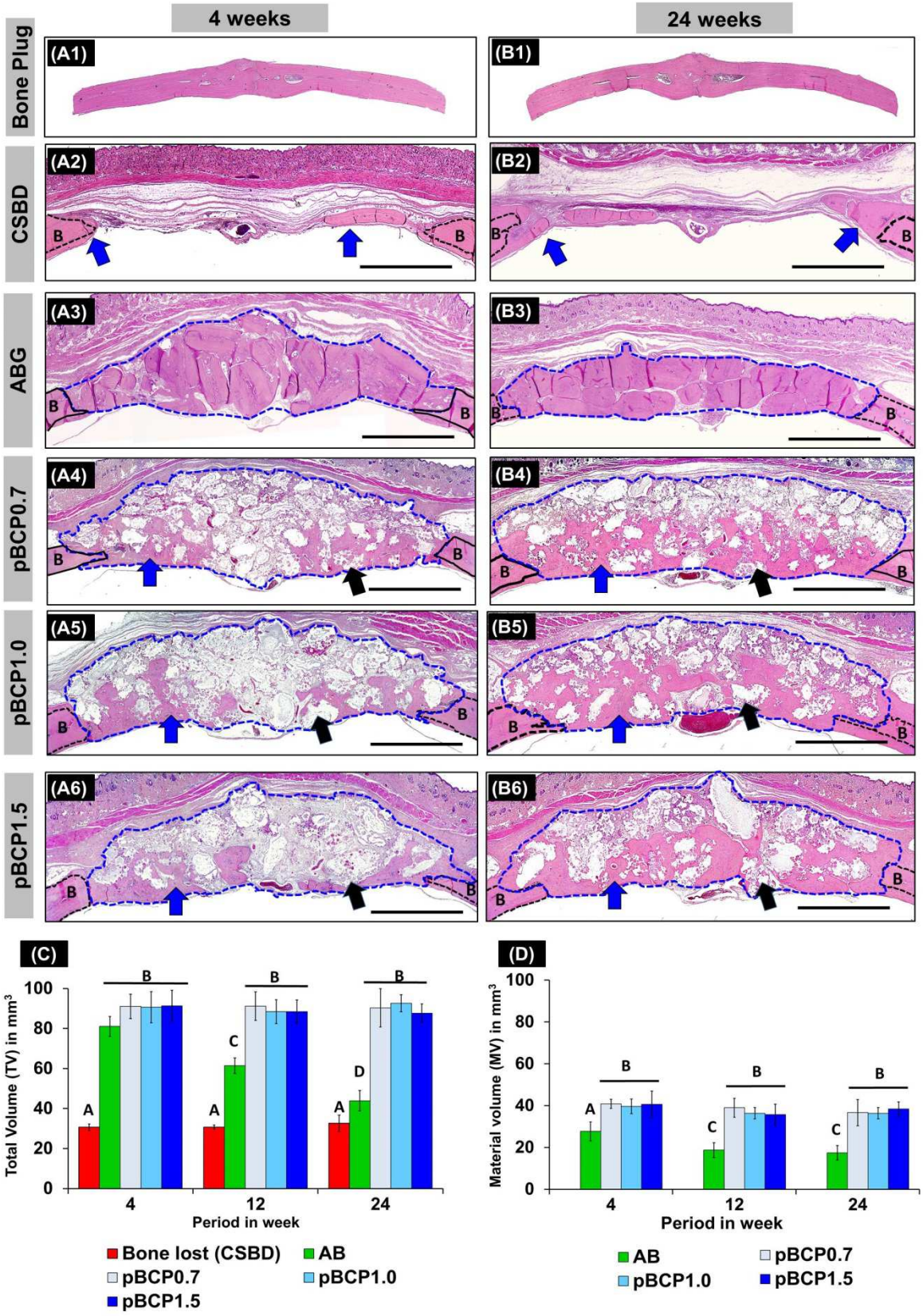
4 weeks
24 weeks
Bone Plug
CSBD
ABG
pBCP0.7
pBCP1.0
pBCP1.5
(A1)
(B1)
(A2)
(B2)
(A3)
(B3)
(A4)
(B4)
(A5)
(B5)
(A6)
(B6)
B
(C)
Total Volume (TV) in mm³
100
80
60
40
20
0
A
B
C
D
4
12
24
Period in week
Bone lost (CSBD)
AB
pBCP0.7
pBCP1.0
pBCP1.5
(D)
Material volume (MV) in mm³

Figure 5

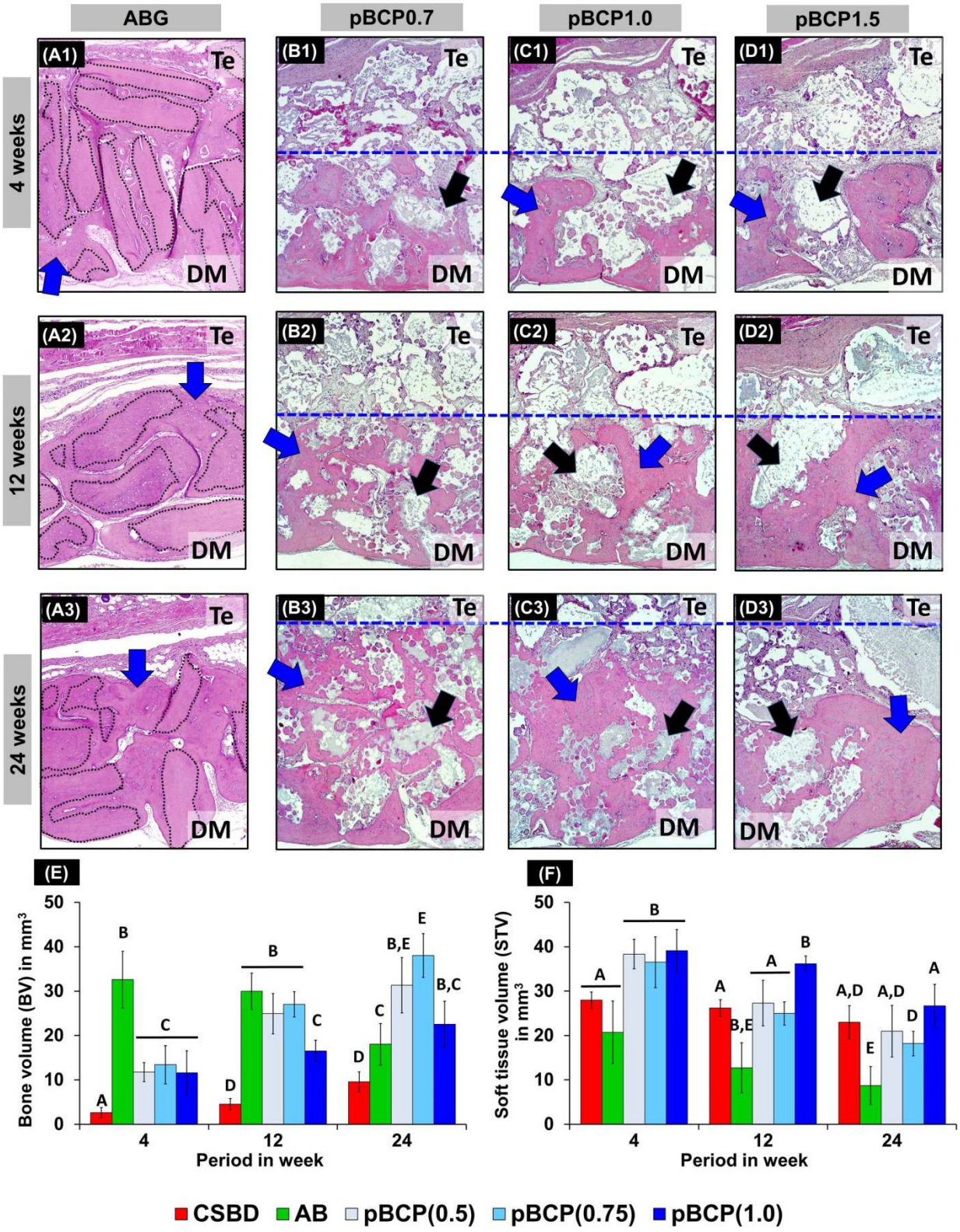
ABG
pBCP0.7
pBCP1.0
pBCP1.5
4 weeks
12 weeks
24 weeks
(A1)
(B1)
(C1)
(D1)
(A2)
(B2)
(C2)
(D2)
(A3)
(B3)
(C3)
(D3)
Te
DM
(E)
Bone volume (BV) in mm³
Period in week
(F)
Soft tissue volume (STV) in mm³
Period in week
CSBD
AB
pBCP(0.5)
pBCP(0.75)
pBCP(1.0)

Figure 6

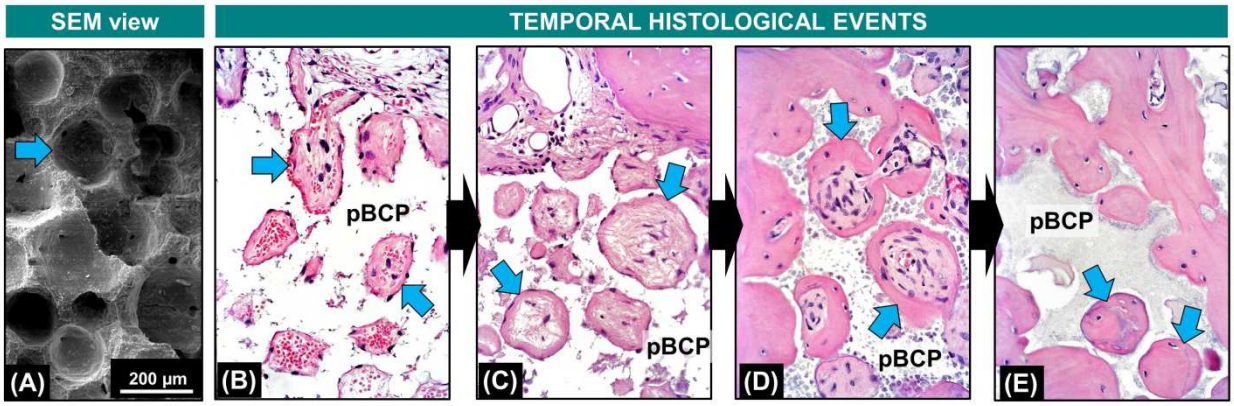
SEM view
TEMPORAL HISTOLOGICAL EVENTS
(A)
200 µm
(B)
pBCP
(C)
pBCP
(D)
pBCP
(E)
pBCP

Figure 7

2.2 ARTICLE 2 – Porous biphasic calcium phosphate ceramic for maxillary sinus floor augmentation: a randomized controlled clinical trial with CBCT, micro-CT and histomorphometry studies

ABSTRACT

Objectives: We aimed to investigate bone regeneration and its volumetric stability after maxillary sinus floor augmentation (MSFA) of the atrophied maxilla treated with novel porous biphasic calcium phosphate (pBCP70:30) in comparison with autogenous bone (AB).

Materials and methods: Bilateral MSFA was performed via lateral wall surgery in twelve patients in a split-mouth design using pBCP70:30 and particulate AB. The volume and height gains were evaluated by three-dimensional (3D) cone beam computed tomography (CBCT) scans obtained at three times: preoperatively (T0), 1 week postoperatively (T1) and 4 months postoperatively (T2). Bone core biopsies were collected during implant placement after 6 months of MSFA. The biopsies were analyzed morphometrically by micro-CT and histology.

Results: The residual ridge height at T0 was 2.3±1.45 mm (p=0.77). At T1, the MSFA volume was higher for pBCP70:30 (1.56±0.8 cm^3) than AB (0.96±0.47 cm^3). At T2, the MSFA volume was similar to that of T1 for pBCP70:30, while for AB, the volume reduced by 31%. The pBCP70:30 and AB core biopsies showed no differences in the bone volume density (30±5.0% vs. 24.5±4.9%, respectively) or residual bone graft (33.1±7.4% vs. 24.6±2.8%, respectively). However, in the pBCP70:30 and AB biopsies, the soft tissue was predominantly connective tissue (25.9±6.9%) and bone marrow (40.8±8.6%), respectively.

Conclusions: The amount of vital bone formed in MSFA with pBCP70:30 and AB is similar. Although the bone repair reaches a more advanced stage with AB, pBCP70:30 promotes greater preservation of the grafted volume than AB and is thus a good alternative for MSFA.

Keywords: Maxillary sinus augmentation; Bone substitute, Biphasic calcium phosphate, autogenous bone; Clinical research

INTRODUCTION

Treatment of the edentulous atrophic maxilla is still a challenge in odontology. Dental implants in the posterior region of an atrophic maxilla represent a compromised mechanical situation of high loading forces in an area with disadvantageous anatomical conditions (Rangert, Sullivan, & Jemt, 1997). Thus, the lack of an adequate quantity of bone after pneumatization of the maxillary sinus makes implant placement difficult, delays treatment and increases the complexity and unpredictability of this therapy (Aparicio, Perales, & Rangert, 2001; Tukel & Tatli, 2018). However, in recent decades, since the introduction of the maxillary sinus floor augmentation (MSFA) surgical technique (Boyne & James, 1980; Smiler et al., 1992), a high rate of success has been achieved.

Traditionally, two sinus floor augmentation techniques are performed with good success rates. First, the transalveolar approach is less invasive and easier to perform with fewer complications, but it may not be indicated for MSFA in cases of a residual ridge height (RRH) less than 5 mm. Second, the lateral window approach, although more invasive, is preferred and indicated in cases of advanced pneumatization with a residual ridge less than 4 mm from the sinus floor. The latter technique may have some complications, but these complications do not decrease the success of the method or the future stability or survival of the implant (de Almeida Ferreira et al., 2017). At this point, the grafting material selected plays a fundamental role in achieving good results with MSFA and may directly influence dental implant success (Hatano, Shimizu, & Ooya, 2004; Jeong & Lee, 2014).

Currently, among bone grafting materials, autogenous bone (AB) is considered the "gold standard" because it presents an excellent combination of three important biological properties (namely, osteoconduction, osteoinduction, and osteogenic capacity) (Miron et al. 2011; Miron et al. 2016). AB is commonly obtained from intraoral and extraoral donor sites and remains the best graft material for bone regeneration (Pereira et al., 2017). However,

clinically, it may have some drawbacks, such as prolonged operating time and hospitalization, increased donor site morbidity, limited availability and susceptibility to infections in staged procedures (Chavda & Levin, 2018). Thus, to overcome these difficulties, surgeons have preferred the use of bone substitutes, such as allografts, xenografts and alloplastic materials (Shanbhag, Shanbhag, & Stavropoulos, 2014).

In this sense, biphasic calcium phosphate (BCP) substitutes containing beta tricalcium phosphate (βTCP) and hydroxyapatite (HA) are good alternatives to AB. The chemical composition of BCP resembles that of the natural inorganic bone matrix; therefore, BCP-based materials show good biocompatibility and osteoconductivity (Frenken et al., 2010). Over 30 years of BCP use, the material has shown good efficacy in many clinical situations, including acting as a scaffold or template and guiding new bone formation (Bouler, Pilet, Gauthier, & Verron, 2017). More recently, it has been observed that some BCP scaffolds can induce ectopic bone formation without the addition of osteoinductive factors, such as BMP2 (Coathup et al., 2012; Santos et al., 2018). This capacity has been attributed to chemical compounds released from the ceramics, such as inorganic Ca^{+2} and phosphate ions, that trigger osteogenic differentiation and subsequently bone formation (Khoshniat et al., 2011; Maeno et al., 2005), but this mechanism is still controversial. Additionally, the physical structural features of these materials, such as the macro- and microporosity, particle size and surface roughness, which vary according to processing parameters, may interfere with their osteoinductive potential (Habibovic & de Groot, 2007; Habibovic et al., 2008). In a previous preclinical study performed by our research group (Santos et al., 2018), a novel porous BCP material containing HA/β-TCP at a 70:30 ratio (pBCP70:30) showed good osteoconductive and osteoinductive properties when implanted in rabbit mandibular critical-size bone defects and heterotopically in mouse thigh muscles. Bone formation occurred into the concavities and macro- and micropores of this graft material, highlighting its osteoinductive potential, which

is directly related to the structural characteristics of a biomaterial (Habibovic & de Groot, 2007; Habibovic et al., 2008).

The present study is the first randomized clinical trial testing the null hypothesis that there are no differences in new bone formation with the use of pBCP70:30 or AB grafts in the treatment of the atrophic maxilla with a lateral approach for MSFA. The alveolar residual ridge dimensions prior to MSFA, as well as the volume and height gains and other volumetric changes after sinus surgery, were monitored by cone beam computed tomography (CBCT). This radiological assessment has gained popularity, and CBCT analyses of MSFA results have been widely reported (Umanjec-Korac, Wu, Hassan, Liu, & Wismeijer, 2014). Additionally, comprehensive micro-CT and histomorphometric analyses of bone core biopsy specimens collected from the grafted area during implant placement were conducted to evaluate the quality and quantity of newly formed bone.

MATERIAL AND METHODS

This study is a prospective, randomized, controlled, clinical trial in a split-mouth design according to the Helsinki protocol. The relevance of this design is that it removes many factors of interindividual variability from the estimates of the therapeutic effect. All procedures were approved by the Ethical Committee for Human Studies (CAAE 03625812.1.0000.5417) of the Bauru School of Dentistry, São Paulo University, Brazil. The CONSORT 2010 guidelines for reporting parallel-group randomized trials were also followed (Schulz, Altman, & Moher, 2010). It was conducted in patients who sought implant treatment in the implant dentistry clinic of the Brazilian Association of Dentists of Balneário Camboriú, Santa Catarina, Brazil, during 2012 and 2013. The clinical study design is illustrated in Figure 1A.

Patient selection

The patients in this study were partially (premolar and molar region) or totally edentulous and all in need of bilateral MSFA. The patients were fully informed about the bone grafting and implant therapy procedures, the benefits and possible risks, and other treatment alternatives and signed a written consent form. The inclusion criteria were as follows: adult subjects aged more than 40 years with total bilateral maxillary atrophy equal to 5 mm or less from the alveolar crest to the sinus floor. The need for sinus elevation was determined by the presence of severe alveolar ridge atrophy rated class IV or V (Cawood & Howell, 1988). Standard exclusion criteria for bone grafting procedures were used, including pregnancy, systemic diseases, allergy, alcoholism, maxillary sinus pathologies (e.g., abscess, cyst and sinusitis), use of illicit drugs or drugs affecting bone metabolism (e.g., steroids and bisphosphonates), recent (within 5 years) radiotherapy in the maxillae, tobacco use, periodontal disease, dentures, and heavily scarred mucosa at the site (Kakar et al., 2017).

Diagnosis was made after a clinical examination and an evaluation of the dental casts and panoramic radiographs to observe the height and width of the alveolar ridge and to identify critical anatomical structures, such as the maxillary sinus and the mandibular canal. A preoperative 3D CBCT examination was also performed to determine the volume needed prior to implant insertion. Additionally, the restorative treatment was planned by occlusal analysis of the articulated casts and diagnostic wax-ups.

Randomization and blinding

A computer-generated list was prepared (http://www.randomizer.org), and concealed randomization envelopes were stored by an independent person unaware of the study protocol. To ensure the blinding, the surgeon did not partake in the statistical analysis. On the other hand, the surgical plan and grouping was confidential to the statistical analyst.

Graft characteristics

AB was harvested from the mandibular ramus and/or symphysis by a surgical procedure under local anesthesia induced using mepivacaine 2% with epinephrine at 1:1000 (DFL, Rio de Janeiro, Brazil). The surgical approaches used Nº 701 burs and chisels, and the harvested bone was crushed by a bone crusher (Muzimed, Canoas, Brazil). The amount of graft to be obtained was determined to fill a volume of approximately 12 mm in height (Fig. 1A). A novel commercially available biphasic ceramic (pBCP70/30; GenPhos-XP, Baumer SA, Mogi Mirim, SP, Brazil) with granulated particles of 0.50-0.75 mm was used in this study (Fig. 1B).

MSFA surgical procedure and biopsy harvesting

All MSFA surgeries were performed by a single well-trained surgeon (RQPM) following the protocol for the lateral window approach (Boyne & James, 1980; Tatum, 1986). Antibiotic prophylaxis (2 g of amoxicillin 1 h before the surgery) and mouth rinsing with chlorhexidine had previously been prescribed to the patients. After local anesthesia was induced with 2% mepivacaine and epinephrine at 1:1000, an incision was made in the mucous membrane 5 mm away from the planned osteotomy, and a full-thickness mucoperiosteal flap was raised. Regarding the contour of the maxillary sinus, as observed in previous X-ray images, a bony window was made in the lateral wall of the sinus using a spherical diamond burr, and then the sinus membrane was released. According to the split-mouth design, both materials were randomly assigned to either the right or left sinus. Thus, after checking the integrity of the Schneiderian membrane with Valsalva maneuver, a sealed opaque envelope was opened, revealing to the surgeon the grafting material to be used. The space created between the membrane and the sinus floor was filled with the graft material, i.e., AB (Fig. 1B1) or pBCP70:30 (Fig. 1B2), randomly selected for the left or right side (Fig. 1B3-1B4) until filling approximately 12 mm of the sinus height (Fig. 1B5-1B6). A resorbable collagen

membrane (GenDerm, BAUMER SA, Mogi Mirim, São Paulo, Brazil) was used to cover the bony window. The primary wound was closed with Vicryl 4-0 (Ethicon, Johnson & Johnson, São José dos Campos, São Paulo, Brazil). Postoperative medication included 550 mg of naproxen sodium for three days and 500 mg of amoxicillin three times daily for seven days to minimize inflammation, relieve/avoid pain and reduce the chances of infection.

At 6 months after MSFA, two hybrid surface implants sandblasted with aluminum oxide particles and etched with acid (Titaniumfix, São José dos Campos, São Paulo, Brazil) were installed in each augmented sinus region. A cylindrical apico-coronal core bone graft biopsy was obtained from the region posterior to the implant using a 3.0 x 15 mm trephine drill (Neodent, Curitiba, Brazil) (Fig. 1B7). The biopsy was then fixed in 10% neutral buffered formalin (pH 7.2) for 48 hours and processed for micro-CT and histomorphometry. Six months later, prosthetic implants were placed.

Radiological analysis

In addition to preoperative panoramic radiographs, 3D CBCT was performed at different time points (see timeline in Fig. 1A). A preoperative (T0) CBCT scan was obtained to evaluate the sinus anatomy, determine the presence of pathologies and examine the residual alveolar ridge. After MSFA surgery, two scans were obtained, one after seven days (T1) and another after four months (T2), to evaluate the grafted volume changes and enhance the precision and accuracy of the implant surgery. All images were obtained using an i-CAT Classic CBCT system (Imaging Sciences International, Hatfield, Pennsylvania, USA). The images were 1.0 mm thick and collected at an interval of 0.2 mm under 120 kVp and 100 mA. CBCT data were collected in the DICOM (Digital Imaging and Communications in Medicine) file format, and 3D analysis was performed using SimPlant OMS Standalone 14.0 software (SIMPLANT Business Unit, Technologielaan, Belgium).

All measurements were repeated two times in new randomized sets by the same investigator. Then, the possible intraexaminer error was tested with postsurgical images from five randomly selected augmented maxillary sinuses. To obtain the gain in height after MSFA (Fig. 1B5-B6), the maximum distance between the alveolar crest and the apical portion of the graft was calculated at T1 and T2 and then compared to the height of the residual alveolar ridge at T0. The volume gains of the grafted materials into the maxillary sinus were calculated according to the "total height method" which consists of subtracting the empty space volume within the maxillary sinus from the total sinus volume (Krennmair, Krainhofner, Maier, Weinlander, & Piehslinger, 2006).

Micro-CT analysis of biopsies

Biopsies obtained with a trephine bur (Fig. 1B7) were scanned by a micro-CT SkyScan 1174 system (Bruker, Aartselaar, Belgium). The X-ray beam source was set to 50 kV and 800 μA, and a 0.5-mm-thick aluminum filter was used. The voxel size was 9.3 μm, and the other parameters included 360° rotation, a rotation step of 1° and three average frames with an exposure time of 5300 ms. Image reconstruction was performed using NRecon 1.6.8 software (Bruker, SkyScan, Aartselaar, Belgium) with the following settings: beam hardening adjustment, 28%; smoothing, 3; ring artifact reduction, 12. Alignment of images in the coronal, sagittal and transaxial planes was performed using DataViewer 1.4.4 software (Bruker, SkyScan, Aartselaar, Belgium). 3D images were obtained using CTVox software (Bruker, SkyScan, Aartselaar, Belgium) (Fig. 2A). In the CTAn program (Bruker, SkyScan, Aartselaar, Belgium), morphometric quantifications of the total volume, bone volume density and grafted material density were performed using a cylindrical region of interest (ROI) 3.1 mm in diameter (Fig. 2B). After volume of interest (VOI) selection, binarization was performed. That is, an image with different gray levels was converted into an image with a

binary representation such that distinguishing the grafted material (Fig. C) from the newly formed bone (Fig. 2D) was possible. Thus, to perform the 3D analysis, adequate threshold ranges were determined for the biomaterial (170-255), the AB (170-255) and the newly formed bone (77-169).

Histological and histomorphometric procedures

Samples were demineralized in EDTA solution containing 4.13% Titriplex III from Merck® and 0.44% sodium hydroxide at 2 to 8 °C for approximately 30 days and then embedded in polymer-enriched paraffin (Histosec, Merck®) Semiserial, 4-µm-thick, apico-coronal and sagittal sections were obtained and stained with hematoxylin and eosin (HE).

The volume density (Vvi) of each constituent (graft, newly formed bone, connective tissue, inflammatory infiltrate and bone marrow) in the biopsy was analyzed in an AxioVision imaging system (Carl Zeiss, Germany). From each biopsy, 4 histological sections were imaged using an AxioScope 2 microscope (Carl Zeiss, Germany) with a 10X objective lens coupled to a high-resolution AxioCam digital camera (Carl Zeiss, Germany). First, the total biopsy area (A) and the total area occupied by each constituent (Ai) were determined. Then, the volume density (Vvi) of each constituent was calculated by the formula VVi = [(Ai/A) x 100] (Weibel, 1969) .

Statistical analysis

InStat software (version 3.0 for Windows) and GraphPad Prism (version 6.0 for Windows) (GraphPad Software Co., La Jolla, CA, USA) were used. Data were checked for normality (Kolmogorov-Smirnov test) and homogeneity (Bartlett test). For CBCT, data were analyzed by paired t test. For micro-CT and histomorphometry, data were analyzed by the Mann-Whitney U test. Correlations between the micro-CT morphometric data and

corresponding histomorphometric values were evaluated using Pearson correlation coefficients (r^2). The significance level was set at 0.05.

RESULTS

Patient and biopsy data

Patient data are shown in Table 1. In all, 12 patients were enrolled in this study according to the eligibility criteria and the power and sample size obtained by Nizam et al. 2018 in a similar clinical model. All patients required bilateral MSFA, and 69 implants were installed in the posterior maxillary region after the surgery. During the MSFA procedure, one Schneiderian membrane in the pBCP70:30 group and another in the AB group perforated. Thus, these two patients were excluded from the study. In addition, eight maxillary sinuses filled with AB and 1 filled with pBCP70:30 did not have enough bone volume to perform the biopsy. Thus, a total of eleven maxillary sinus biopsies were collected during the implant installation period, 3 from the AB group and 8 from the pBCP70:30 group.

CBCT analysis

CBCT analysis of the maxillary sinuses (Fig. 3) of 12 patients showed a similar RRH between the groups at T0 (mean height, 2.3 mm). Seven days after MSFA (T1), the presence of the grafted material was observed on both the right and left sides, but the grafted volume was greater in the pBCP70:30 (1.56 cm^3) group than in the AB (0.96 cm^3) group. At 4 months after MSFA (T2), the grafted volume of AB was reduced by 31%, while that of pBCP70:30remained stable. At T2, the maximum gain in height (T2-T0) was not significantly different between the groups (see radiographic images and morphometric data in Fig. 3).

Micro-CT and histomorphometry analyses of the biopsies

Histological sections show an excellent, high-resolution representation of the bone, soft tissues and cells, while micro-CT provides a 3D view of the mineralized structures at the microscopic level. Thus, the 3D reconstructed micro-CT images obtained were compared with representative images of histological sections, as illustrated in Figures 4-6.

In all biopsies in the AB group (Fig. 4), both micro-CT and histological images showed the presence of large, dense particles of AB surrounded by a thin low-density layer of newly formed bone (NB), with the spaces between them filled with soft tissue. Histologically, the AB particles presented a lamellar bone tissue pattern with many nutrient channels and empty osteocyte lacunae. The thin, newly formed woven bone around the particles presented a disorganized arrangement, with several dispersed osteocytes in the bone matrix without a lamellar arrangement. The hypodense black spaces between the particles and newly formed bone shown in the micro-CT images were filled with bone marrow.

In all biopsies in the pBCP70:30 group, both micro-CT and histological images (Figs. 5-6) showed the presence of pBCP70:30 granules with irregular shapes and contours. Inside the pores and concavities of granules and in the spaces between them, a large amount of newly formed bone was observed that partially (Fig. 5B2) or totally (Fig. 5B1) filled the spaces. In all samples, newly formed bone was in direct contact with the residual grafting material. Histologically, six pBCP70:30 biopsies showed newly formed cancellous bone with a lamellar arrangement, without signs of bone or biomaterial resorption and with large spaces between the particles filled by bone marrow bone and connective tissue (Fig. 5). In the other three biopsies, dense new bone formation was observed filling large parts of the spaces between the particles, along with several giant multinucleated cells and/or osteoclasts on the surface of the pBCP70:30 granules and newly formed bone, indicating active remodeling of

both the bone and the grafted material (Fig. 6). In these cases, the small spaces observed between the bone trabeculae and pBCP70:30 granules were filled by connective tissue.

3D micro-CT morphometry and 2D histomorphometry

Table 2 shows the morphometric data obtained by micro-CT and histology. The Mann-Whitney U test did not show significant differences between the groups regarding the total volume of the biopsy according to the 3D micro-CT analysis or the volume density of the graft material and newly formed bone according to either evaluation method. The volume density distributions obtained by the histomorphometric and microtomographic analyses (Fig. 7) show a high positive Pearson's correlation coefficient for both the graft material (Fig. 7A, $r^2 = 0.72$) and newly formed bone (Fig. 7B, $r^2 = 0.77$). The connective tissue volume density obtained from the histological sections was significantly higher in the pBCP70:30 group than in the AB group, whereas the bone marrow volume density was significantly lower (see Table 2).

DISCUSSION

The present randomized clinical trial compared the clinical performance of pBCP70:30 and AB grafts in MSFA prior to the placement of dental implants. To date, the best material for bone regeneration and reconstruction is AB (Pereira et al., 2017); nevertheless, pBCP70:30 has been shown to be an efficient substitute for bone autografts. Based on the results obtained by CBCT, 3D micro-CT and histomorphometry, we provide evidence supporting acceptance of the null hypothesis that there are no differences in new bone formation between pBCP70:30 and AB treatments in MSFA in the short term. In addition, pBCP70:30 showed optimal clinical performance due to its lower graft volume loss than AB and high bioactivity.

Both AB and pBCP70:30 performed successfully, with 83% of patients (10 of 12 patients) experiencing uneventful treatment. However, 17% of patients experienced membrane perforation in one sinus, and this rate is within the current range, i.e., 20% to 24%, for sinus membrane perforation occurring with the use of rotatory instruments (Jordi, Mukaddam, Lambrecht, & Kuhl, 2018; Stacchi et al., 2017). This most common intraoperative complication of MSFA is related to anatomical factors, such as septa, the thickness and angles of sinus walls and mucosal membrane abnormalities (Shanbhag, Karnik, Shirke, & Shanbhag, 2014; Tukel & Tatli, 2018). Additionally, a residual bone height of 3-6 mm with the presence of septa is associated with membrane perforation and graft failure (Becker et al., 2008; Tukel & Tatli, 2018). No other complications, such as bleeding or infection, occurred. A collagen membrane was used to cover the lateral window to reduce the chances of sinus infection and to increase graft survival (Pjetursson, Tan, Zwahlen, & Lang, 2008).

In the present study, the RRH as evaluated by CBCT at T0 was 2.3 mm, which is below the current range of 4.9 mm to 8.6 mm recently reported by others using CBCT (Lozano-Carrascal et al., 2017). This RRH observed in our patients strictly indicated that the lateral window approach for MSFA was more suitable than the transalveolar technique (Shanbhag, Karnik, et al., 2014). Moreover, in these cases, other approaches present a higher risk of failure (Pjetursson et al., 2008). The vertical grafted height at T2 was similar between the groups (9.4 mm for pBCP70:30 and 9.2 mm for AB) and provided enough bone to achieve primary stability with high-torque implant insertion (≥45 N) after 6 months of healing. Similar height gains have also been found among other grafting materials, e.g., 8.5 mm to 11 mm with xenografts (Fouad, Osman, Atef, & Hakam, 2018; Umanjec-Korac et al., 2014), and 8.7 mm (Frenken et al., 2010) and 7.5 mm (Bouwman, Bravenboer, Frenken, Ten Bruggenkate, & Schulten, 2017) with BCP60:40 after 6 and 9 months, respectively.

Graft resorption and sinus repneumatization can occur after MSFA to different degrees among different materials after different periods of time (Hatano et al., 2004). To assess the graft volume and determine the rate of reabsorption, CBCT is widely used because it is practical and allows accurate 3D evaluation (Umanjec-Korac et al., 2014). In the present study, CBCT showed a significant loss of 31% of the AB graft volume at T2. Comparatively, previous CBCT studies have noted AB graft volume reductions ranging from 16% to 49% at 6 months. These variations may be influenced by the donor harvesting site (Johansson, Grepe, Wannfors, & Hirsch, 2001; Smolka, Eggensperger, Carollo, Ozdoba, & Iizuka, 2006). In this regard, higher graft volume reductions could be a disadvantage of using AB, since in cases of infection or graft failure, replacement using AB would not be possible (Nkenke & Neukam, 2014). In contrast, the pBCP70:30 volume did not change. Since previous clinical studies using BCP60:40 have shown a reduction of approximately 15% of volume at six months (Kuhl et al., 2013; Ohe et al., 2016), the volume maintenance observed for pBCP70:30 can be explained by the HA/TCP ratio.

The presence of high bioactivity is an important factor that determines the rate of graft turnover, i.e., graft remodeling, which permits live tissue formation around the graft. Thus, biopsies harvested during implant installation were analyzed by micro-CT and histomorphometry. A strong Pearson correlation coefficient ($r > 0.8$) was observed between the volume density data obtained by both methods for both the graft material and the newly formed bone. The concomitant use of micro-CT and histology provided a comprehensive picture of the quality and quantity of bone regenerated at 6 months after MSFA surgery. Although the volume density of the pBCP70:30 granules (33.05%) was higher than that of the AB particles (24.57%), no significant differences were found ($p=0.0636$). The same result was observed for the volume density of newly formed bone, with a tendency toward higher values for MSFA with pBCP70:30 (30%) than that with AB (24.5%). The favorable bone

formation associated with pBCP70:30 may be due to its osteoinductive property (Santos et al., 2018). It should be noted that other studies using BCP60:40 have also shown new bone formation ranging from 21% to 30% and no differences with the use of AB compared with deproteinized bovine bone (Cordaro et al., 2008; Danesh-Sani et al., 2016; Froum, Wallace, Cho, Elian, & Tarnow, 2008). In contrast, Danesh-Sani et al. (2016) showed a significantly higher volume of newly formed bone for AB (36.8%) than for BCP60/40 (28.2%) and an average of 32.9% and 4.8% residual graft particles, respectively (Danesh-Sani et al., 2016). In the abovementioned work, the rapid AB graft resorption could be due to the graft origin in the zygomatic buttress, lateral sinus wall or tuberosity area, all of which have porous cortical bone with fine trabeculae (D3 and D4 Misch classifications). In the present work, the AB originated from the mentum or ramus of the mandible, each of which is principally composed of dense cortical bone (D1 and D2 Misch classifications). These different AB remodeling rates clearly indicate that the AB donor site directly influences both the remodeling rate and new bone formation.

On the other hand, the histological sections showed a higher degree of bone maturation in the AB group than the pBCP70:30 group. The AB core biopsies were filled with large cortical bone graft particles surrounded by new lamellar bone, with the spaces between them occupied by bone marrow. In the pBCP70:30 biopsies, connective tissue filled most of the spaces between the particles, and intense bone remodeling by osteoclasts was observed in some samples. Multinucleated giant cells/osteoclasts involved in the resorption/remodeling of both the bone and grafted material were found around the pBCP70:30 granules. These results agree with those of previous reports; therefore, AB remains the “gold standard” for bone regeneration (Danesh-Sani, Engebretson, & Janal, 2017; Sakkas, Wilde, Heufelder, Winter, & Schramm, 2017).

CONCLUSION

The CBCT, 3D micro-CT and histomorphometric results obtained in this randomized clinical trial indicate that pBCP70:30 is a good osteoconductive graft material that promotes a similar amount of bone formation as does AB and loses less graft volume than AB in patients undergoing MSFA procedures, as evaluated over the short term. The biopsy features were also similar for both materials, despite the pBCP70:30 showing more soft tissue and less bone marrow formation. Clinically, the two materials displayed similar bioactivity and bone remodeling rate, while the pBCP70:30 exhibited higher total volume maintenance. Additional studies are needed to evaluate the long-term performance of pBCP70:30 in MSFA.

Acknowledgments

The authors thank the Associação Brasileira de Cirurgiões Dentistas (ABCD, Balneário Camboriú, SC, Brazil) for providing access to patients and dental clinics for the performance of MSFA and Odonto Imagem Radiologia (Balneário Camboriú, SC, Brazil) for providing CBCT radiological support for this study. The authors also thank Baumer SA (Mogi Mirim, SP, Brazil) for providing GenPhos-XP and Titaniumfix (AS Technology, Campos do Jordão, SP, Brazil) for donating the dental implants used in this study.

Conflicts of interest

The authors declare that there are no conflicts of interest regarding the publication of this paper.

REFERENCES

Aparicio, C., Perales, P., & Rangert, B. (2001). Tilted implants as an alternative to maxillary sinus grafting: a clinical, radiologic, and periotest study. Clin Implant Dent Relat Res, 3(1), 39-49.

Becker, S. T., Terheyden, H., Steinriede, A., Behrens, E., Springer, I., & Wiltfang, J. (2008). Prospective observation of 41 perforations of the Schneiderian membrane during sinus floor elevation. Clin Oral Implants Res, 19(12), 1285-1289. doi:10.1111/j.1600-0501.2008.01612.x

Bouler, J. M., Pilet, P., Gauthier, O., & Verron, E. (2017). Biphasic calcium phosphate ceramics for bone reconstruction: A review of biological response. Acta Biomater, 53, 1-12. doi:10.1016/j.actbio.2017.01.076

Bouwman, W. F., Bravenboer, N., Frenken, J., Ten Bruggenkate, C. M., & Schulten, E. (2017). The use of a biphasic calcium phosphate in a maxillary sinus floor elevation procedure: a clinical, radiological, histological, and histomorphometric evaluation with 9- and 12-month healing times. Int J Implant Dent, 3(1), 34. doi:10.1186/s40729-017-0099-x

Boyne, P. J., & James, R. A. (1980). Grafting of the maxillary sinus floor with autogenous marrow and bone. J Oral Surg, 38(8), 613-616.

Cawood, J. I., & Howell, R. A. (1988). A classification of the edentulous jaws. Int J Oral Maxillofac Surg, 17(4), 232-236.

Chavda, S., & Levin, L. (2018). Human Studies of Vertical and Horizontal Alveolar Ridge Augmentation Comparing Different Types of Bone Graft Materials: A Systematic Review. J Oral Implantol, 44(1), 74-84. doi:10.1563/aaid-joi-D-17-00053

Coathup, M. J., Hing, K. A., Samizadeh, S., Chan, O., Fang, Y. S., Campion, C., . . . Blunn, G. W. (2012). Effect of increased strut porosity of calcium phosphate bone graft

substitute biomaterials on osteoinduction. Journal of Biomedical Materials Research Part A, 100A(6), 1550-1555. doi:10.1002/jbm.a.34094

Cordaro, L., Bosshardt, D. D., Palattella, P., Rao, W., Serino, G., & Chiapasco, M. (2008). Maxillary sinus grafting with Bio-Oss or Straumann Bone Ceramic: histomorphometric results from a randomized controlled multicenter clinical trial. Clin Oral Implants Res, 19(8), 796-803. doi:10.1111/j.1600-0501.2008.01565.x

Danesh-Sani, S. A., Engebretson, S. P., & Janal, M. N. (2017). Histomorphometric results of different grafting materials and effect of healing time on bone maturation after sinus floor augmentation: a systematic review and meta-analysis. J Periodontal Res, 52(3), 301-312. doi:10.1111/jre.12402

Danesh-Sani, S. A., Wallace, S. S., Movahed, A., El Chaar, E. S., Cho, S. C., Khouly, I., & Testori, T. (2016). Maxillary Sinus Grafting With Biphasic Bone Ceramic or Autogenous Bone: Clinical, Histologic, and Histomorphometric Results From a Randomized Controlled Clinical Trial. Implant Dent, 25(5), 588-593. doi:10.1097/id.0000000000000474

de Almeida Ferreira, C. E., Martinelli, C. B., Novaes, A. B., Jr., Pignaton, T. B., Guignone, C. C., Goncalves de Almeida, A. L., & Saba-Chujfi, E. (2017). Effect of Maxillary Sinus Membrane Perforation on Implant Survival Rate: A Retrospective Study. Int J Oral Maxillofac Implants, 32(2), 401-407. doi:10.11607/jomi.4419

Fouad, W., Osman, A., Atef, M., & Hakam, M. (2018). Guided maxillary sinus floor elevation using deproteinized bovine bone versus graftless Schneiderian membrane elevation with simultaneous implant placement: Randomized clinical trial. Clin Implant Dent Relat Res. doi:10.1111/cid.12601

Frenken, J. W., Bouwman, W. F., Bravenboer, N., Zijderveld, S. A., Schulten, E. A., & ten Bruggenkate, C. M. (2010). The use of Straumann Bone Ceramic in a maxillary sinus

floor elevation procedure: a clinical, radiological, histological and histomorphometric evaluation with a 6-month healing period. Clin Oral Implants Res, 21(2), 201-208. doi:10.1111/j.1600-0501.2009.01821.x

Froum, S. J., Wallace, S. S., Cho, S. C., Elian, N., & Tarnow, D. P. (2008). Histomorphometric comparison of a biphasic bone ceramic to anorganic bovine bone for sinus augmentation: 6- to 8-month postsurgical assessment of vital bone formation. A pilot study. Int J Periodontics Restorative Dent, 28(3), 273-281.

Habibovic, P., & de Groot, K. (2007). Osteoinductive biomaterials--properties and relevance in bone repair. J Tissue Eng Regen Med, 1(1), 25-32. doi:10.1002/term.5

Habibovic, P., Kruyt, M. C., Juhl, M. V., Clyens, S., Martinetti, R., Dolcini, L., van Blitterswijk, C. A. (2008). Comparative in vivo study of six hydroxyapatite-based bone graft substitutes. J Orthop Res, 26(10), 1363-1370. doi:10.1002/jor.20648

Hatano, N., Shimizu, Y., & Ooya, K. (2004). A clinical long-term radiographic evaluation of graft height changes after maxillary sinus floor augmentation with a 2:1 autogenous bone/xenograft mixture and simultaneous placement of dental implants. Clin Oral Implants Res, 15(3), 339-345. doi:10.1111/j.1600-0501.2004.00996.x

Jeong, T. M., & Lee, J. K. (2014). The Efficacy of the Graft Materials after Sinus Elevation: Retrospective Comparative Study Using Panoramic Radiography. Maxillofacial Plastic and Reconstructive Surgery, 36(4), 146-153. doi:10.14402/jkamprs.2014.36.4.146

Johansson, B., Grepe, A., Wannfors, K., & Hirsch, J. M. (2001). A clinical study of changes in the volume of bone grafts in the atrophic maxilla. Dentomaxillofac Radiol, 30(3), 157-161. doi:10.1038/sj/dmfr/4600601

Jordi, C., Mukaddam, K., Lambrecht, J. T., & Kuhl, S. (2018). Membrane perforation rate in lateral maxillary sinus floor augmentation using conventional rotating instruments and

piezoelectric device-a meta-analysis. Int J Implant Dent, 4(1), 3. doi:10.1186/s40729-017-0114-2

Kakar, A., Rao, B. H. S., Hegde, S., Deshpande, N., Lindner, A., Nagursky, H., . . . Mahajan, H. (2017). Ridge preservation using an in situ hardening biphasic calcium phosphate (β-TCP/HA) bone graft substitute—a clinical, radiological, and histological study. In Int J Implant Dent (Vol. 3).

Khoshniat, S., Bourgine, A., Julien, M., Weiss, P., Guicheux, J., & Beck, L. (2011). The emergence of phosphate as a specific signaling molecule in bone and other cell types in mammals. Cell Mol Life Sci, 68(2), 205-218. doi:10.1007/s00018-010-0527-z

Krennmair, G., Krainhofner, M., Maier, H., Weinlander, M., & Piehslinger, E. (2006). Computerized tomography-assisted calculation of sinus augmentation volume. Int J Oral Maxillofac Implants, 21(6), 907-913.

Kuhl, S., Brochhausen, C., Gotz, H., Filippi, A., Payer, M., d'Hoedt, B., & Kreisler, M. (2013). The influence of bone substitute materials on the bone volume after maxillary sinus augmentation: a microcomputerized tomography study. Clin Oral Investig, 17(2), 543-551. doi:10.1007/s00784-012-0732-2

Lozano-Carrascal, N., Salomo-Coll, O., Gehrke, S. A., Calvo-Guirado, J. L., Hernandez-Alfaro, F., & Gargallo-Albiol, J. (2017). Radiological evaluation of maxillary sinus anatomy: A cross-sectional study of 300 patients. Ann Anat, 214, 1-8. doi:10.1016/j.aanat.2017.06.002

Maeno, S., Niki, Y., Matsumoto, H., Morioka, H., Yatabe, T., Funayama, A., . . . Tanaka, J. (2005). The effect of calcium ion concentration on osteoblast viability, proliferation and differentiation in monolayer and 3D culture. Biomaterials, 26(23), 4847-4855. doi:10.1016/j.biomaterials.2005.01.006

Nkenke, E., & Neukam, F. W. (2014). Autogenous bone harvesting and grafting in advanced jaw resorption: morbidity, resorption and implant survival. Eur J Oral Implantol, 7 Suppl 2, S203-217.

Ohe, J. Y., Kim, G. T., Lee, J. W., Al Nawas, B., Jung, J., & Kwon, Y. D. (2016). Volume stability of hydroxyapatite and beta-tricalcium phosphate biphasic bone graft material in maxillary sinus floor elevation: a radiographic study using 3D cone beam computed tomography. Clin Oral Implants Res, 27(3), 348-353. doi:10.1111/clr.12551

Pereira, R. S., Gorla, L. F., Boos, F., Okamoto, R., Garcia Junior, I. R., & Hochuli-Vieira, E. (2017). Use of autogenous bone and beta-tricalcium phosphate in maxillary sinus lifting: histomorphometric study and immunohistochemical assessment of RUNX2 and VEGF. Int J Oral Maxillofac Surg, 46(4), 503-510. doi:10.1016/j.ijom.2017.01.002

Pjetursson, B. E., Tan, W. C., Zwahlen, M., & Lang, N. P. (2008). A systematic review of the success of sinus floor elevation and survival of implants inserted in combination with sinus floor elevation. J Clin Periodontol, 35(8 Suppl), 216-240. doi:10.1111/j.1600-051X.2008.01272.x

Rangert, B. R., Sullivan, R. M., & Jemt, T. M. (1997). Load factor control for implants in the posterior partially edentulous segment. Int J Oral Maxillofac Implants, 12(3), 360-370.

Sakkas, A., Wilde, F., Heufelder, M., Winter, K., & Schramm, A. (2017). Autogenous bone grafts in oral implantology-is it still a "gold standard"? A consecutive review of 279 patients with 456 clinical procedures. Int J Implant Dent, 3(1), 23. doi:10.1186/s40729-017-0084-4

Santos, P. S., Cestari, T. M., Paulin, J. B., Martins, R., Rocha, C. A., Arantes, R. V. N., . . . Taga, R. (2018). Osteoinductive porous biphasic calcium phosphate ceramic as an alternative to autogenous bone grafting in the treatment of mandibular bone critical-

size defects. J Biomed Mater Res B Appl Biomater, 106(4), 1546-1557. doi:10.1002/jbm.b.33963

Schulz, K. F., Altman, D. G., & Moher, D. (2010). CONSORT 2010 statement: updated guidelines for reporting parallel group randomized trials. Ann Intern Med, 152(11), 726-732. doi:10.7326/0003-4819-152-11-201006010-00232

Shanbhag, S., Karnik, P., Shirke, P., & Shanbhag, V. (2014). Cone-beam computed tomographic analysis of sinus membrane thickness, ostium patency, and residual ridge heights in the posterior maxilla: implications for sinus floor elevation. Clin Oral Implants Res, 25(6), 755-760. doi:10.1111/clr.12168

Shanbhag, S., Shanbhag, V., & Stavropoulos, A. (2014). Volume changes of maxillary sinus augmentations over time: a systematic review. Int J Oral Maxillofac Implants, 29(4), 881-892. doi:10.11607/jomi.3472

Smiler, D. G., Johnson, P. W., Lozada, J. L., Misch, C., Rosenlicht, J. L., Tatum, O. H., Jr., & Wagner, J. R. (1992). Sinus lift grafts and endosseous implants. Treatment of the atrophic posterior maxilla. Dent Clin North Am, 36(1), 151-186; discussion 187-158.

Smolka, W., Eggensperger, N., Carollo, V., Ozdoba, C., & Iizuka, T. (2006). Changes in the volume and density of calvarial split bone grafts after alveolar ridge augmentation. Clin Oral Implants Res, 17(2), 149-155. doi:10.1111/j.1600-0501.2005.01182.x

Stacchi, C., Andolsek, F., Berton, F., Perinetti, G., Navarra, C. O., & Di Lenarda, R. (2017). Intraoperative Complications During Sinus Floor Elevation with Lateral Approach: A Systematic Review. Int J Oral Maxillofac Implants, 32(3), e107-e118. doi:10.11607/jomi.4884

Tatum, H., Jr. (1986). Maxillary and sinus implant reconstructions. Dent Clin North Am, 30(2), 207-229.

Tukel, H. C., & Tatli, U. (2018). Risk factors and clinical outcomes of sinus membrane perforation during lateral window sinus lifting: analysis of 120 patients. Int J Oral Maxillofac Surg. doi:10.1016/j.ijom.2018.03.027

Umanjec-Korac, S., Wu, G., Hassan, B., Liu, Y., & Wismeijer, D. (2014). A retrospective analysis of the resorption rate of deproteinized bovine bone as maxillary sinus graft material on cone beam computed tomography. Clin Oral Implants Res, 25(7), 781-785. doi:10.1111/clr.12174

Weibel, E. R. (1969). Stereological principles for morphometry in electron microscopic cytology. Int Rev Cytol, 26, 235-302.

Table 1. Patients and biopsies data

Number of enrolled patients	12
Females/male	10/2
Mean of age ± SD, years (range)	50 ± 6 (37-63)
Right maxilla	8 AB 4 pBCP70:30
Left maxilla	4 AB 8 pBCP70:30
Total number of implants (range)	69 (2-8 per patient)
Number of bone biopsy	3 AB 9 pBCP70:30
Mean biopsy height	4.04±0.76 mm for AB 5.81±1.62 mm for pBCP70:30

Table 2. Mean ± standard deviation (SD); range and p-value of the Mann-Whitney test of data obtained from 3D-microCT morphometry (CTAn software) and bidimensional (2D) histomorphometry of the biopsies.

Parameters Mean ± SD (range)	AB (n=3)	pBCP70:30 (n=9)	Mann-Whitney U Test (p value)
Micro-CT morphometry			
Biopsy total volume TV (mm^3)	39.64 ± 10.91 (28.67–50,49)	53.00 ± 15.22 (35.51–81.44)	0.2818
Graft materials volume density GmV/TV (%)	26.79 ± 3.11 (23.25–28.01)	30.22 ± 7.91 (20.03–42.92)	0.5791
Newly formed bone volume NbV/TV (%)	24.71 ± 3.90 (24.59–28.66)	32.87 ± 5.73 (27.07-42.86)	0.0961
Histomorphometry			
Graft materials volume density GmV/TV (%)	24.57 ± 2.75 (22.12–27.55)	33.05 ± 7.37 (23.62-44.33)	0.0785
Newly formed bone volume density NbV/TV (%)	24.50 ± 4.90 (19.04–28.52)	30.45 ± 5.00 (23.83–36.18)	0.2091
Connective tissue volume density CTV/TV (%)	10.17 ± 6.19 (3.48–15.69)	25.90 ± 6.93 (17.15–34.37)	**0.0182**
Marrow bone Volume density BMV/TV (%)	40.76 ± 8.60 (30.83–45.88)	10.18 ± 8.97 (1.51-21.43)	**0.0091**

Figure legends

Figure 1. Clinical study design (A): Timeline showing the period of patient selection between 2012 and 2013, the MSFA surgical procedure (T0), the acquisition of CBCT images at 15 days before MSFA (T0), 7 days after MSFA (T1), and 4 months after MSFA (T2), and biopsy collection with concomitant implant installation at six months after MSFA. Bilateral MSFA procedures and biopsy harvesting (B): (A) Particulate AB. B) pBCP70:30 granules. (C-D) Right and left bony windows created in the antero-lateral wall of the maxilla with one sinus filled with AB (C) and the contralateral sinus filled with pBCP70:30 (D). (E-F) Tomographic assessment of the maxillary sinus cavities filled with AB (E) and pBCP70:30 (F). (G) Trephine biopsy after MSFA.

Figure 2. Micro-CT reconstruction and analysis of bone graft biopsies: (A) 3D sagittal view showing particles of AB (blue arrow) and pBCP70:30 (yellow arrow) involved with newly formed bone (red arrow) and the assessed VOI (dotted area blue). (B) 2D coronal view of biopsies showing density differences among the AB (blue arrow), pBCP70:30 (yellow arrow) and newly formed bone (red arrow). (C) Binary images used to distinguish the graft materials, AB and pBCP70:30 (salmon color), from new bone (green color). (D) Binary images used to distinguish of newly formed bone (salmon color) from the graft materials (green color).

Figure 3. CBCT images and analysis of MSFA with AB and pBCP70:30. A panoramic view (PV) and oblique sagittal cross section of the right (R) and left (L) sinuses of a male (EB) and female (ES) patient at different time points. T0 (preoperative) images showing the RRH between the crestal level (blue line) and the sinus floor level (yellow line). At T1 (7 days after MSFA) and T2 (4 months after MSFA), the grafted area of the MS appears as a

hyperdense area; the gain in height is marked by a red line. The table shows the mean and SD of the height and grafted volume in MSFA with pBCP70:30 and AB, as determined by CBCT, and their p values obtained by paired t test.

Figure 4. Micro-CT and histological images of a biopsy after MSFA with autogenous bone harvested at 6 months: (A) Sagittal micro-CT image showing newly formed bone (red arrow) as low-density areas around higher-density AB particles (blue arrow). (B) Corresponding panoramic histological image. (B1 and B2) Details of (B) showing large AB particles (area surrounded by black dotted line) with empty osteocytic lacunae surrounded by a thin layer of newly formed bone (red arrow). Note the new bone formation (green arrow) around the AB nutritional channels (Au) and that the spaces between the particles are filled by bone marrow (BM). HE staining, 10X and 100X.

Figure 5. Micro-CT and histological images of a biopsy after MSFA with pBCP70:30 harvested at 6 months: (A) Sagittal micro-CT image showing the fine trabeculae of newly formed bone (red arrow) as low-density areas surrounding higher-density pBCP70:30 granules (blue arrow). (B) Corresponding panoramic histological image. (B1 and B2) Details showing new bone formation around a pBCP70:30 granule (red arrow in B1) and inside concavities (red arrow B2). Note that the spaces between the granules are filled by connective tissue (CT) and bone marrow (BM). HE staining, 10X and 100X.

Figure 6. Micro-CT and histological images of a biopsy after MSFA with pBCP70:30 harvested at 6 months showing graft/bone turnover: (A) Sagittal micro-CT image of a biopsy showing the thick trabeculae of newly formed bone as hipo-dense areas (red arrow) occupying the spaces between high-density pBCP70:30 granules (blue arrow). (B)

Corresponding panoramic histological image. (B1 and B2) Details show extensive bone formation on the pBCP70:30 granule surface. Note the presence of multinucleated giant cells/osteoclasts (black arrows) on the bone and pBCP70:30 surfaces. HE staining, 10X and 100X.

Figure 7. Pearson correlation graphs for graft material volume density (A) and newly formed bone (B) obtained by micro-CT and histology. The graph shows the trend line obtained by combining both techniques, the equation, and the resulting coefficients of correlation (r) and determination (r^2).

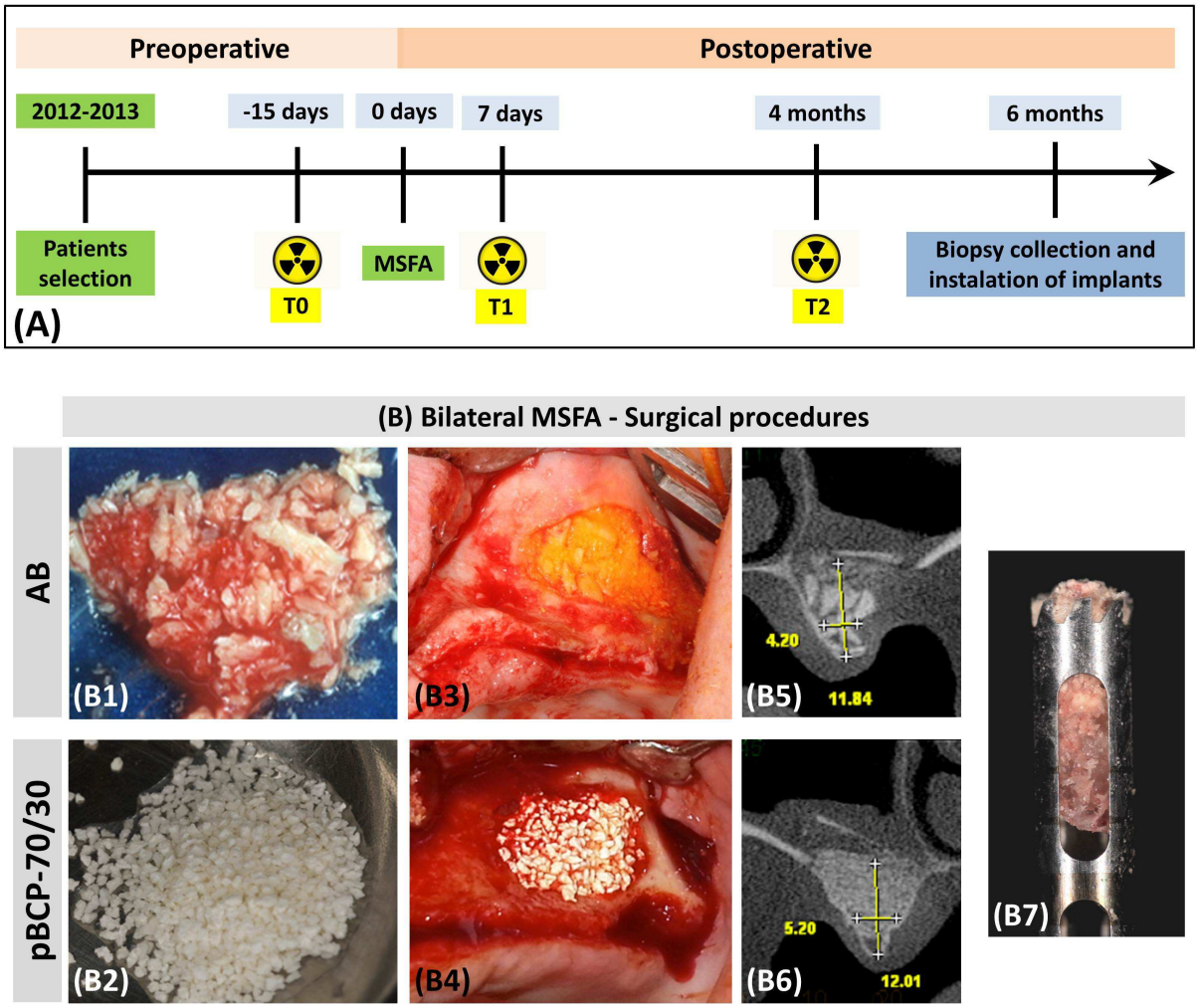
Preoperative
Postoperative
2012-2013
-15 days
0 days
7 days
4 months
6 months
Patients selection
T0
MSFA
T1
T2
Biopsy collection and instalation of implants
(A)
(B) Bilateral MSFA - Surgical procedures
AB
pBCP-70/30
(B1)
(B2)
(B3)
(B4)
(B5)
4.20
11.84
(B6)
5.20
12.01
(B7)

Figure 1

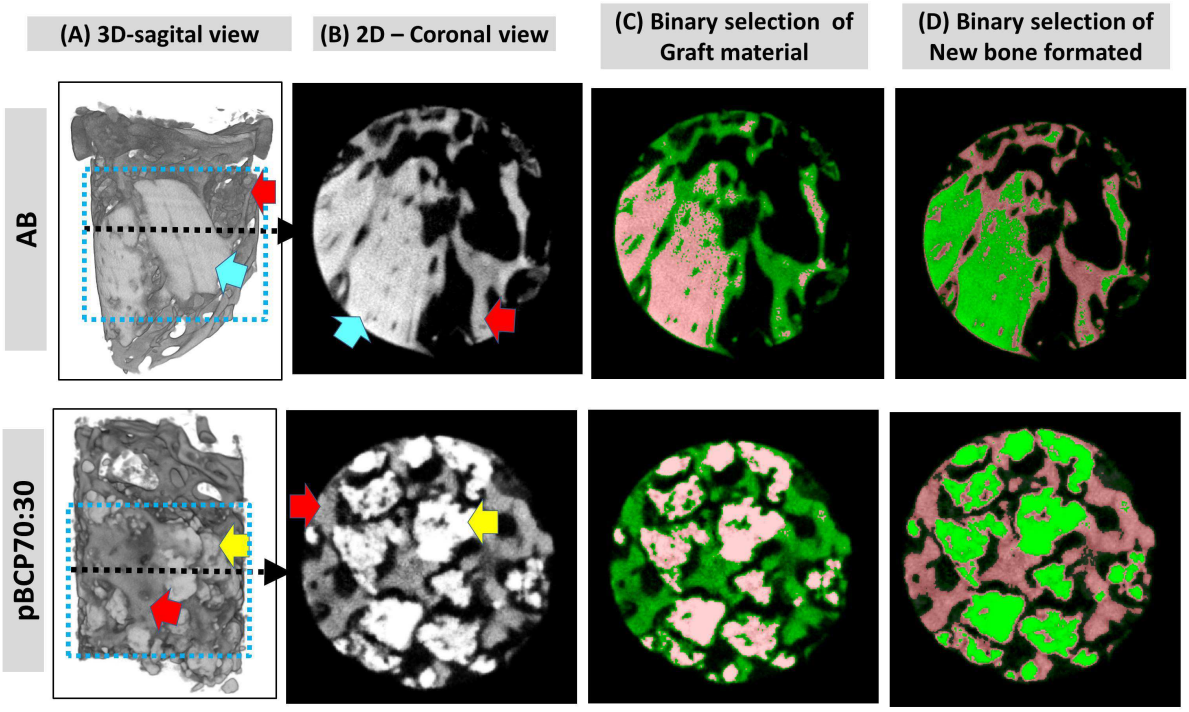
(A) 3D-sagital view
(B) 2D – Coronal view
(C) Binary selection of Graft material
(D) Binary selection of New bone formated
AB
pBCP70:30

Figure 2

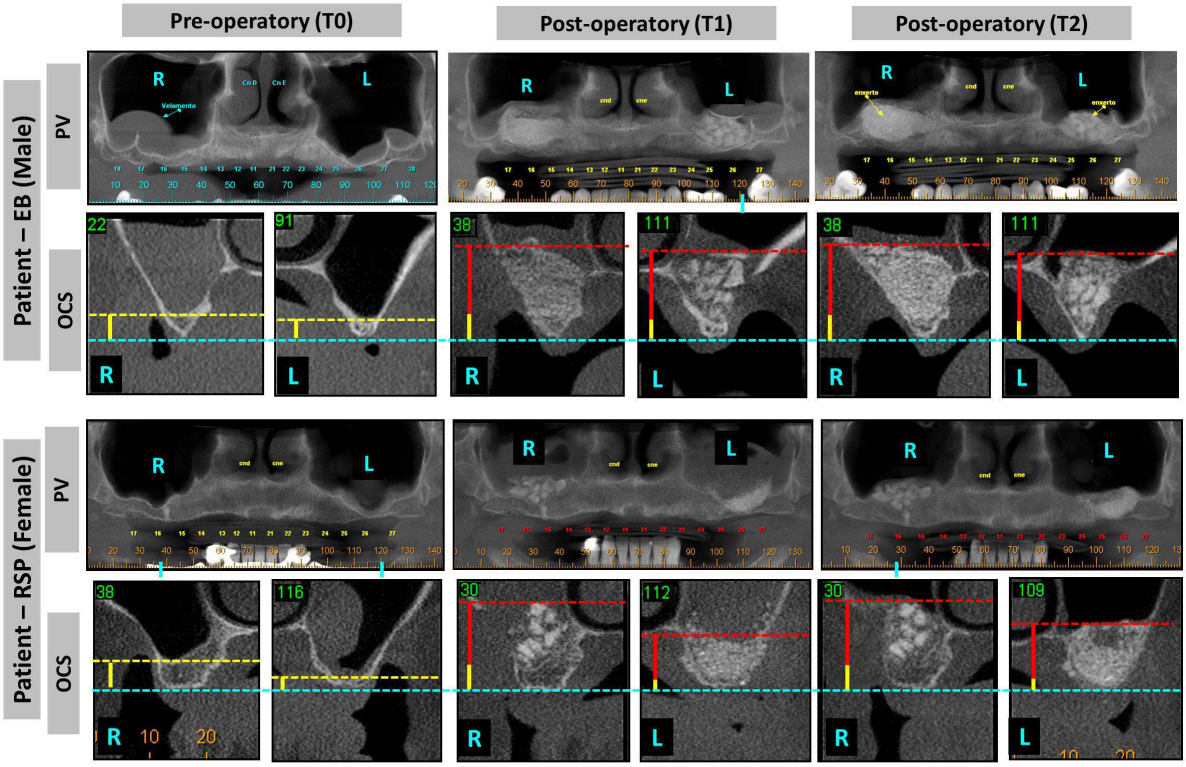

Group	Height in mm (Range)		Grafted volume in cm^3 (Range)		
	RRH (T0)	Maximum gain (T2-T0)	T1	T2	Paired test "t" (p-values)
AB	2.21 ± 1.53 (0.47 – 4.95)	9.18 ± 2.58 (4.80 – 12.13)	0.960 ± 0.456 (0.347 – 1.914)	0.665 ± 0.327 (0.175 – 1.201)	0.0001
pBCP70:30	2.4 ± 1.14 (0.84 - 4.06)	9.36 ± 2.85 (5.27-14.30)	1.556 ± 0.803 (0.409 – 2.866)	1559.1 ± 0.842 (0.392 – 3.111)	0.9895
Paired test "t" (p-values)	0.7747	0.8636	0.0092	0.0012	

Figure 3

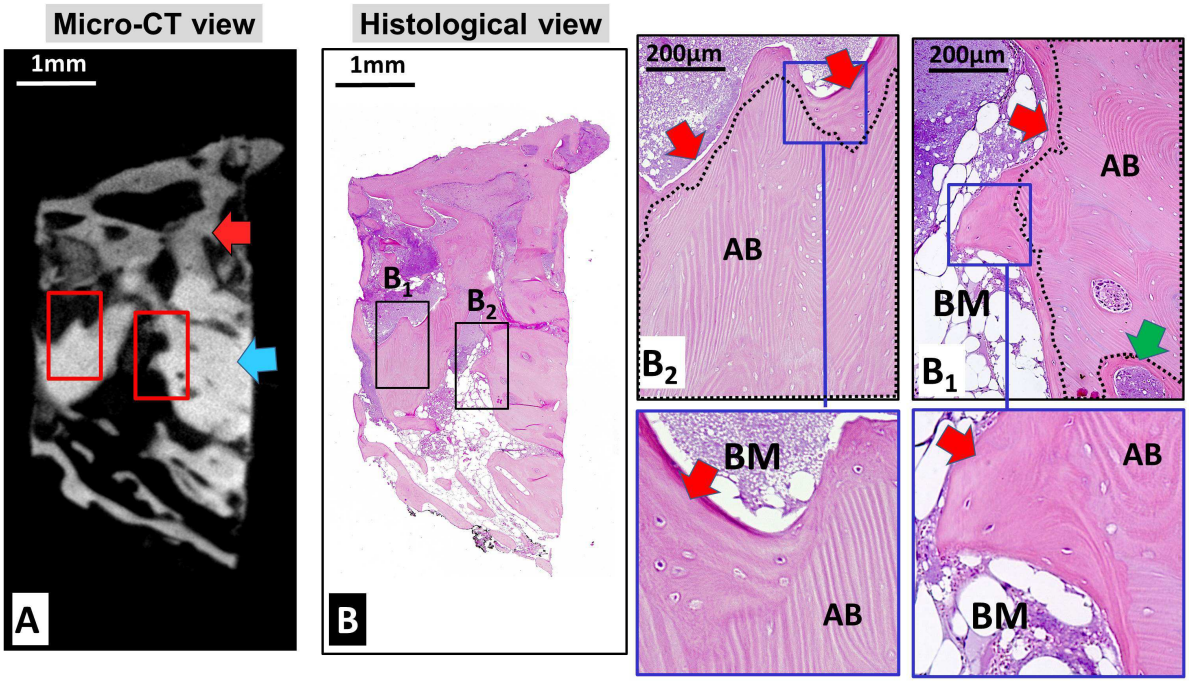
Micro-CT view
Histological view
1mm
1mm
A
B
B1
B2
200µm
200µm
AB
AB
BM
B2
B1
BM
AB
AB
BM

Figure 4

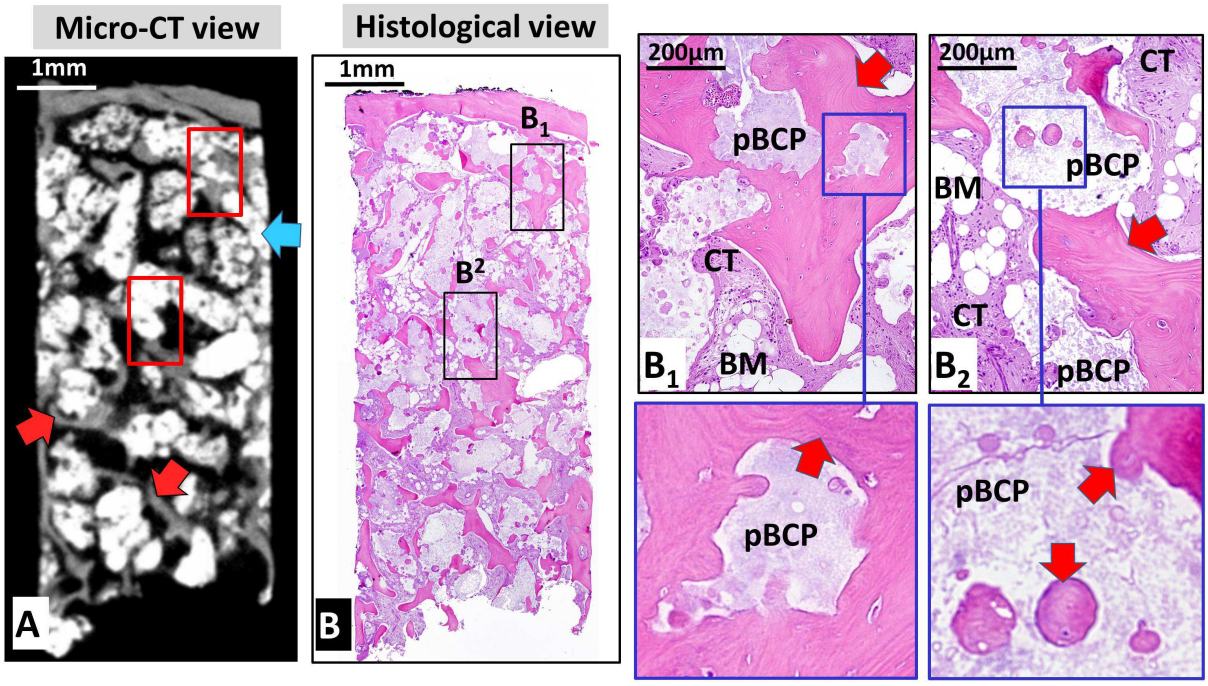
Micro-CT view
Histological view
1mm
1mm
A
B
B1
B2
200µm
200µm
pBCP
CT
BM
pBCP
CT
BM
CT
pBCP
pBCP

Figure 5

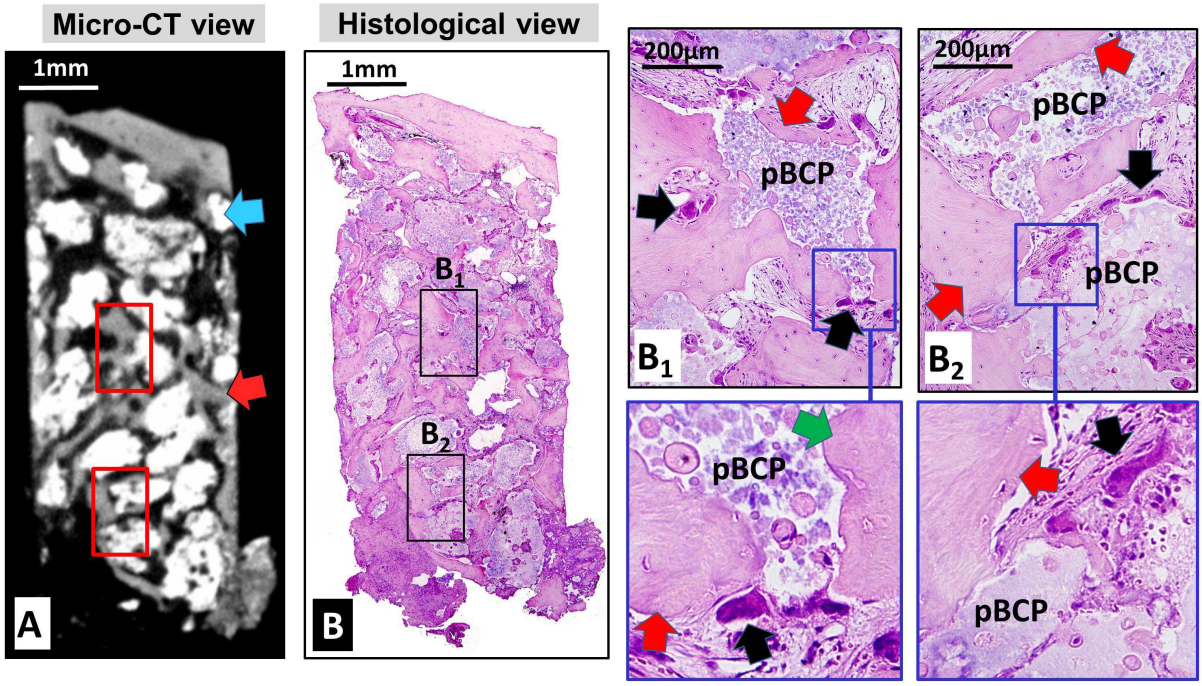
Micro-CT view
Histological view
1mm
1mm
A
B
B1
B2
200µm
200µm
pBCP
pBCP
pBCP
pBCP
pBCP
B1
B2

Figure 6

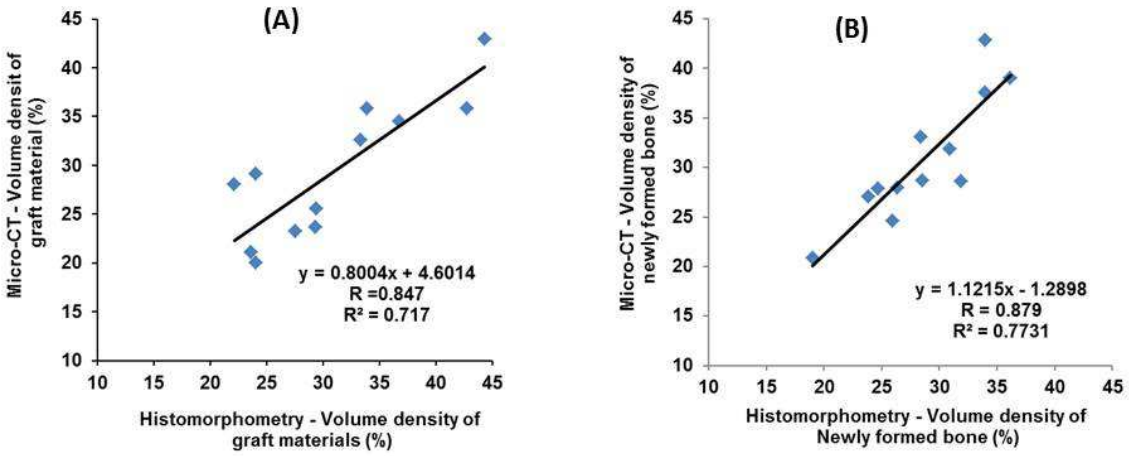
(A)
Micro-CT - Volume densit of graft material (%)
y = 0.8004x + 4.6014
R =0.847
R² = 0.717
Histomorphometry - Volume density of graft materials (%)
(B)
Micro-CT - Volume density of newly formed bone (%)
y = 1.1215x - 1.2898
R = 0.879
R² = 0.7731
Histomorphometry - Volume density of Newly formed bone (%)

Figure 7

3 DISCUSSION

3 DISCUSSION

AB remains as the gold standard for bone regeneration (Sakkas *et al.*, 2017). In the present research, the porous HA/TCP-70/30 bone ceramic showed a bioactivity and bone formation similar to autogenous bone AB in the preclinical critical sized defect model in rats and maxillary sinus augmentation procedures in patients. Both approaches showed particular bone formation in different regions within the grafted area, highlighting the higher osteoconductive potential of this pBCP. Moreover, in the clinical approach, a good graft stability, i.e., low graft remodeling rate, during maxillary sinus augmentation and prior to dental implant placement, was observed in the short term. Physicochemical characteristics of both HA and β-TCP phases in the preclinical approach appeared stable among the different granular sizes of 0.7, 1.0 and 1.5 mm. All granular sizes showed more graft stability than AB in the long term (4-24 weeks). However, the 1.5 mm pBCP was less stable and less advantageous in promoting bone formation than other granule sizes. We found a similar performance of porous HA/TCP:7030 to AB as a bone substitute for bone regeneration in the preclinical critical size defect model and maxillary sinus floor augmentation procedure in patients.

According to our outcomes, bone formation promotion between AB and pBCP/70:30 appeared similar in the clinical approach in the short term. However, in the preclinical approach and long term, granular sizes of 0.7 and 1 mm promoted more bone formation than AB and 1.5 mm was equal to the latter. Additionally, differences in the quality of bone formation were clearly observed and most of these differences were related to the common properties of the biomaterial (osteoinductivity, osteoconductivity and osteogenenicity). This is seen in the host tissue response to the biomaterial used.

The outcomes of articles 1 and 2 are in agreement with the current literature (Vos *et al.*, 2009; Sakkas *et al.*, 2017; Chavda and Levin, 2018), considering AB as the gold standard for bone regeneration. At this point, AB displayed all the three main properties of a bone grafting substitute and it was evidenced by the presence of newly formed bone around AB particles in all regions within the grafted area. Although it could not be seen in the clinical approach (MSFA), because of its short-term design and the impossibility of harvesting more than one bone graft core biopsy, it was more evident in the preclinical approach in the long term (figure 5, 1st article). On the other hand, pBCP/70:30 showed to be more osteconductive than osteoinductive (Habibovic *et al.*, 2008; Tortamano *et al.*, 2012; Wang *et al.*, 2015). Thus, bone formation occurred around the BCP granule surfaces locally, but in a panoramic view, the bone was formed from the border toward the center of the defects and also from the duramater side toward the teguments (figure 5, 12st article). A previous study from our research group analyzed HA/TCP 70/30 implanted in mandibular critical size defects and within muscle bundles and reported new bone formation over their surface, pores and concavities (Santos *et al.*, 2018). While comparing granules size of this BCP, different microenvironments were stablished that may explain the differences in bone formation rate among the granular size groups. Thus, our outcomes support that bone formation rate is affected by pBCP granular variations. Besides, we also consider that proper physicochemical characterization of a biomaterial must be performed as an integral part of the *in vivo* testing studies (Ebrahimi *et al.*, 2017).

In some clinical situations, such as sinus augmentation (MSFA), graft volume stability is necessary (Kirmeier *et al.*, 2008; Kuhl *et al.*, 2015), which means that low resorption rate is desired in such cases. On this issue, AB showed to be less advantageous than pBCP/70:30, since its higher resorption rate led to graph volume diminution, which can affect the total volume needed for the implant placement. HA/TCP ratios are adjusted to obtain a proper

balance between the resorption time of the scaffold and the timing of new bone formation in specific clinical situations (Jensen *et al.*, 2009; Mangano *et al.*, 2015; Helder *et al.*, 2018). The low rate of pBCP/70:30 biodegradability is explained by the higher proportion of HA content versus β-TCP. Regarding this graft stability, in a mandibular defect model, AB graft can be comparable to BCP 20/80, whereas BCP 60/40 and BCP 80/20 rather equaled the known as ‘‘bone substitute control’’ DBBM xenograft (Jensen *et al.*, 2009). In MSFA procedure, BCP 60/40 showed an 84.32% graft volume maintenance until a short-term post-op of 6 months (Ohe *et al.*, 2016). Addition of AB to BCP 60/40 also increased its reabsorption rate from 15% to 18% after six months of MSFA (Kuhl *et al.*, 2015). Our clinical results pointed a significant higher grafted sinus volume maintenance by pBCP/70:30 (85%) vs AB (70%). However, AB resorption rate relies on the quality of the donor area. The cancellous AB from extraoral sites usually has a high resorption rate and leads to minimal bone formation (Block and Kent, 1997; Block *et al.*, 1998). In the preclinical approach, critical size defect model (Article 1), grafted volume reduction of AB reached 45% in the long term. On the other hand, the differences in granular size of pBCP/70:30 (0.7 mm, 1.0 mm and 1.5 mm) did not influence the total grafted volume maintenance, which was far higher than AB at 24 weeks. In spite of pBCP volume maintenance, 1.5-mm granules group showed significant graft volume reduction versus other granular size groups, indicating that there might not be a direct relationship between granular size stability and volume maintenance.

In bone substitutes studies, animal experimentation is a better approach than in vitro tests, and usage of animal models is often essential in extrapolating the experimental results and translating the information into a human clinical setting (Bigham-Sadegh and Oryan, 2015). Critical size defect in rats still represents a reliable preclinical model to analyze bone regeneration. Despite clinical studies are far more significant, sample size and other factors such as variability of individuals may represent a difficulty for them. In the clinical approach,

a self-controlled study design known as split-mouth study is preferred because it eliminates most of the sources of bias that occur in similar controlled studies (Al-Almaie *et al.*, 2017). Core biopsies are limited and represent a challenge in the clinical practice;, once performed they provide valuable data regarding other factors that influence MSFA than implant placement and survival (Kirmeier *et al.*, 2008).

In summary, pBCPs seem to be good substitutes to treat bone loss. Moreover, in Dentistry ceramic bone substitutes and autografts show more acceptance and preference among patients when compared to allografts and xenografts (Fernández *et al.*, 2015). Both preclinical and clinical approaches support that pBCP/70:30 having similar bioactivity to AB, while promoting bone formation and higher graft stability. Granular size points potential influence on the biomaterial performance, however this topic deserves further analyses in specific clinical conditions. For the clinical practice, to get a predictable MSFA outcome, precise measurement methods of the grafted area would be one of the important factors for successful implant treatment, because loss of graft height and width might compromise the future implants placement into the grafted maxilla (Ohe *et al.*, 2016). More studies are still necessary to get a more comprehensive panorama regarding graft stability and granular size influence on bone regeneration processes.

4 CONCLUSIONS

4 CONCLUSIONS

In conclusion, this study demonstrated:

- The novel BCP evaluated in this study is a ceramic biphasic formatted by hydroxyapatite and β-TCP in a 70/30 ratio. This material contains several concavities and micropores on its surface, increasing surface area for bone deposition and a Ca/P ration of 1.8.
- The presence of concavities in pBCP surface creates a favorable microenvironment for bone formation, which is directly influenced by the granule size. Small and medium granule size of pBCP promoted higher bone gain than large size in an 8-mm critical bone defect in rat skull.
- In the preclinical model, although AB graft showed a higher bone gain at the shorter period (4 weeks), this gain was not maintained at longer periods (12 and 24 weeks), while the slow absorption of pBCP favored the bone ingrowth until 24 weeks at higher values than AB.
- Clinically, pBCP promoted a similar amount of bone formation and less loss of graft volume when compared to AB in patients undergoing MSFA procedures in the short term (six months).
- Thus, pBCP might be an efficient bone substitute to repair large bone defects and to promote bone augmentation, as an alternative to autologous bone.

REFERENCES

REFERENCES

AGHALOO, T. L.; MOY, P. K. Which hard tissue augmentation techniques are the most successful in furnishing bony support for implant placement? **Int J Oral Maxillofac Implants,** v. 22 Suppl, p. 49-70, 2007. ISSN 0882-2786 (Print)0882-2786. Available at: < http://dx.doi.org/ >.

AL-ALMAIE, S. et al. A Split-Mouth Design Comparison for Lateral and Crestal Sinus Lift Techniques with Dental Implants Placements: Short Communication. **Open Dent J,** v. 11, p. 603-608, 2017. ISSN 1874-2106 (Print)1874-2106. Available at: < http://dx.doi.org/10.2174/1874210601711010603 >.

BIGHAM-SADEGH, A.; ORYAN, A. Selection of animal models for pre-clinical strategies in evaluating the fracture healing, bone graft substitutes and bone tissue regeneration and engineering. **Connect Tissue Res,** v. 56, n. 3, p. 175-94, Jun 2015. ISSN 0300-8207. Available at: < http://dx.doi.org/10.3109/03008207.2015.1027341 >.

BLOCK, M. S.; KENT, J. N. Sinus augmentation for dental implants: the use of autogenous bone. **J Oral Maxillofac Surg,** v. 55, n. 11, p. 1281-6, Nov 1997. ISSN 0278-2391 (Print)0278-2391.

BLOCK, M. S. et al. Bone maintenance 5 to 10 years after sinus grafting. **J Oral Maxillofac Surg,** v. 56, n. 6, p. 706-14; discussion 714-5, Jun 1998. ISSN 0278-2391 (Print)0278-2391. Available at: < http://dx.doi.org/ >.

BODIC, F. et al. Bone loss and teeth. **Joint Bone Spine,** v. 72, n. 3, p. 215-21, May 2005. ISSN 1297-319X (Print) 1297-319x.

BOULER, J. M. et al. Biphasic calcium phosphate ceramics for bone reconstruction: A review of biological response. **Acta Biomater,** v. 53, p. 1-12, Apr 15 2017. ISSN 1742-7061. Available at: < http://dx.doi.org/10.1016/j.actbio.2017.01.076 >.

BOYNE, P. J.; JAMES, R. A. Grafting of the maxillary sinus floor with autogenous marrow and bone. **J Oral Surg,** v. 38, n. 8, p. 613-6, Aug 1980. ISSN 0022-3255 (Print)0022-3255. Available at: < http://dx.doi.org/ >.

CHAVDA, S.; LEVIN, L. Human Studies of Vertical and Horizontal Alveolar Ridge Augmentation Comparing Different Types of Bone Graft Materials: A Systematic Review. **J Oral Implantol,** v. 44, n. 1, p. 74-84, Feb 2018. ISSN 0160-6972. Available at: < http://dx.doi.org/10.1563/aaid-joi-D-17-00053 >.

CHEN, Z. et al. **Osteoimmunomodulation for the development of advanced bone biomaterials**. 2015.

CHOW, L. C. Development of Self-Setting Calcium Phosphate Cements. **Journal of the Ceramic Society of Japan,** v. 99, n. 1154, p. 954-964, 1991.

CHRCANOVIC, B.; ALBREKTSSON, T.; WENNERBERG, A. **Bone Quality and Quantity and Dental Implant Failure: A Systematic Review and Meta-analysis**. 2017.

COATHUP, M. J. et al. The effect of particle size on the osteointegration of injectable silicate-substituted calcium phosphate bone substitute materials. **J Biomed Mater Res B Appl Biomater,** v. 101, n. 6, p. 902-10, Aug 2013. ISSN 1552-4973. Available at: < http://dx.doi.org/10.1002/jbm.b.32895 >.

_____. Effect of increased strut porosity of calcium phosphate bone graft substitute biomaterials on osteoinduction. **Journal of Biomedical Materials Research Part A,** v. 100A, n. 6, p. 1550-1555, 2012/06/01 2012. ISSN 1549-3296. Available at: < https://doi.org/10.1002/jbm.a.34094 >. Accessed on: 2018/08/24.

DACULSI, G. et al. Osteoconduction, Osteogenicity, Osteoinduction, what are the fundamental properties for a smart bone substitutes. **IRBM,** v. 34, n. 4, p. 346-348, 2013/11/01/ 2013. ISSN 1959-0318. Available at: < http://www.sciencedirect.com/science/article/pii/S1959031813000808 >.

DACULSI, G.; LEGEROS, R. **Biphasic calcium phosphate (BCP) bioceramics: Chemical, physical and biological properties**. 2006. 1-9.

DONGO, V. et al. Lateral sinus floor elevation without grafting materials. Individual- and aggregate-data meta-analysis. **J Craniomaxillofac Surg,** v. 46, n. 9, p. 1616-1624, Sep 2018. ISSN 1010-5182.

DOROZHKIN, S. V. Biphasic, triphasic and multiphasic calcium orthophosphates. **Acta Biomater,** v. 8, n. 3, p. 963-77, Mar 2012. ISSN 1742-7061. Available at: < http://dx.doi.org/10.1016/j.actbio.2011.09.003 >.

EBRAHIMI, M.; BOTELHO, M. G.; DOROZHKIN, S. V. Biphasic calcium phosphates bioceramics (HA/TCP): Concept, physicochemical properties and the impact of standardization of study protocols in biomaterials research. **Mater Sci Eng C Mater Biol Appl,** v. 71, p. 1293-1312, Feb 1 2017. ISSN 0928-4931. Available at: < http://dx.doi.org/10.1016/j.msec.2016.11.039 >.

FERNÁNDEZ, R. F. et al. Bone grafts utilized in dentistry: an analysis of patients' preferences. **BMC Medical Ethics,** v. 16, p. 71, 10/20 09/05/received

07/14/accepted 2015. ISSN 1472-6939. Available at: < http://www.ncbi.nlm.nih.gov/pmc/articles/PMC4618514/ >.

HABIBOVIC, P. et al. Comparative in vivo study of six hydroxyapatite-based bone graft substitutes. **J Orthop Res,** v. 26, n. 10, p. 1363-70, Oct 2008. ISSN 0736-0266.

_____. 3D microenvironment as essential element for osteoinduction by biomaterials. **Biomaterials,** v. 26, n. 17, p. 3565-3575, 2005/06/01/ 2005. ISSN 0142-9612. Available at: < http://www.sciencedirect.com/science/article/pii/S014296120400883X >.

HELDER, M. N. et al. Evaluation of a new biphasic calcium phosphate for maxillary sinus floor elevation: Micro-CT and histomorphometrical analyses. **Clin Oral Implants Res,** v. 29, n. 5, p. 488-498, May 2018. ISSN 0905-7161. Available at: < http://dx.doi.org/10.1111/clr.13146 >.

HING, K. A. et al. Microporosity enhances bioactivity of synthetic bone graft substitutes. **Journal of Materials Science: Materials in Medicine,** v. 16, n. 5, p. 467-475, 2005/05/01 2005. ISSN 1573-4838. Available at: < https://doi.org/10.1007/s10856-005-6988-1 >.

JENSEN, S. S. et al. Comparative study of biphasic calcium phosphates with different HA/TCP ratios in mandibular bone defects. A long-term histomorphometric study in minipigs. **J Biomed Mater Res B Appl Biomater,** v. 90, n. 1, p. 171-81, Jul 2009. ISSN 1552-4973. Available at: < http://dx.doi.org/10.1002/jbm.b.31271 >.

JORDANA, F.; LE VISAGE, C.; WEISS, P. [Bone substitutes]. **Med Sci (Paris),** v. 33, n. 1, p. 60-65, Jan 2017. ISSN 0767-0974.

KIRMEIER, R. et al. Evaluation of three-dimensional changes after sinus floor augmentation with different grafting materials. **Clin Oral Implants Res,** v. 19, n. 4, p. 366-72, Apr 2008. ISSN 0905-7161.

KUHL, S. et al. The influence of particulated autogenous bone on the early volume stability of maxillary sinus grafts with biphasic calcium phosphate: a randomized clinical trial. **Clin Implant Dent Relat Res,** v. 17, n. 1, p. 173-8, Feb 2015. ISSN 1523-0899.

KUMAR, P.; VINITHA, B.; FATHIMA, G. Bone grafts in dentistry. **J Pharm Bioallied Sci,** v. 5, n. Suppl 1, p. S125-7, Jun 2013. ISSN 0976-4879 (Print)0975-7406. Available at: < http://dx.doi.org/10.4103/0975-7406.113312 >.

MANGANO, C. et al. A Human Clinical, Histological, Histomorphometrical, and Radiographical Study on Biphasic HA-Beta-TCP 30/70 in Maxillary Sinus Augmentation. **Clin Implant Dent Relat Res,** v. 17, n. 3, p. 610-8, Jun 2015. ISSN 1523-0899. Available at: < http://dx.doi.org/10.1111/cid.12145 >.

MARTIN, W.; LEWIS, E.; NICOL, A. Local risk factors for implant therapy. **Int J Oral Maxillofac Implants,** v. 24 Suppl, p. 28-38, 2009. ISSN 0882-2786 (Print) 0882-2786.

MCALLISTER, B. S.; HAGHIGHAT, K. Bone augmentation techniques. **J Periodontol,** v. 78, n. 3, p. 377-96, Mar 2007. ISSN 0022-3492 (Print)0022-3492.

MOHAN, N.; WOLF, J.; DYM, H. Maxillary sinus augmentation. **Dent Clin North Am,** v. 59, n. 2, p. 375-88, Apr 2015. ISSN 0011-8532.

OHE, J. Y. et al. Volume stability of hydroxyapatite and beta-tricalcium phosphate biphasic bone graft material in maxillary sinus floor elevation: a radiographic study using 3D cone beam computed tomography. **Clin Oral Implants Res,** v. 27, n. 3, p. 348-53, Mar 2016. ISSN 0905-7161. Available at: < http://dx.doi.org/10.1111/clr.12551 >.

PAL, U. S. et al. Direct vs. indirect sinus lift procedure: A comparison. **Natl J Maxillofac Surg,** v. 3, n. 1, p. 31-7, Jan 2012. ISSN 0975-5950 (Print)0975-5950. Available at: < http://dx.doi.org/10.4103/0975-5950.102148 >.

POLO-CORRALES, L.; LATORRE-ESTEVES, M.; RAMIREZ-VICK, J. E. Scaffold design for bone regeneration. **J Nanosci Nanotechnol,** v. 14, n. 1, p. 15-56, Jan 2014. ISSN 1533-4880 (Print) 1533-4880.

PRINS, H. J. et al. Spatial distribution and survival of human and goat mesenchymal stromal cells on hydroxyapatite and beta-tricalcium phosphate. **J Tissue Eng Regen Med,** v. 10, n. 3, p. 233-44, Mar 2016. ISSN 1932-6254. Available at: < http://dx.doi.org/10.1002/term.1681 >.

SAKKAS, A. et al. Autogenous bone grafts in oral implantology-is it still a "gold standard"? A consecutive review of 279 patients with 456 clinical procedures. **Int J Implant Dent,** v. 3, n. 1, p. 23, Dec 2017. ISSN 2198-4034 (Print)2198-4034. Available at: < http://dx.doi.org/10.1186/s40729-017-0084-4 >.

SANTOS, P. S. et al. Osteoinductive porous biphasic calcium phosphate ceramic as an alternative to autogenous bone grafting in the treatment of mandibular bone critical-size defects. **J Biomed Mater Res B Appl Biomater,** v. 106, n. 4, p. 1546-1557, May 2018. ISSN 1552-4973. Available at: < http://dx.doi.org/10.1002/jbm.b.33963 >.

SHARAN, A.; MADJAR, D. Maxillary sinus pneumatization following extractions: a radiographic study. **Int J Oral Maxillofac Implants,** v. 23, n. 1, p. 48-56, Jan-Feb 2008. ISSN 0882-2786 (Print)0882-2786. Available at: < http://dx.doi.org/ >.

SHIBUYA, N.; JUPITER, D. C. Bone graft substitute: allograft and xenograft. **Clin Podiatr Med Surg,** v. 32, n. 1, p. 21-34, Jan 2015. ISSN 0891-8422.

TORTAMANO, A. et al. Periodontopathogens around the surface of mini-implants removed from orthodontic patients. **Angle Orthod,** v. 82, n. 4, p. 591-5, Jul 2012. ISSN 0003-3219. Available at: < http://dx.doi.org/10.2319/081011-506.1 >.

VEREECKE, G.; LEMAÎTRE, J. Calculation of the solubility diagrams in the system Ca(OH)2-H3PO4-KOH-HNO3-CO2-H2O. **Journal of Crystal Growth,** v. 104, n. 4, p. 820-832, 1990/09/01/ 1990. ISSN 0022-0248. Available at: < http://www.sciencedirect.com/science/article/pii/002202489090108W >.

VOS, M. D. et al. Autogenous femoral head as grafting material for mandibular augmentation. **International Journal of Oral and Maxillofacial Surgery,** v. 38, n. 12, p. 1320-1323, 2009. ISSN 0901-5027. Available at: < http://www.embase.com/search/results?subaction=viewrecord&from=export&id=L50653513 >.Available at: < http://dx.doi.org/10.1016/j.ijom.2009.09.002 >.

WANG, L. et al. Effect of particle size on osteoinductive potential of microstructured biphasic calcium phosphate ceramic. **J Biomed Mater Res A,** v. 103, n. 6, p. 1919-29, Jun 2015. ISSN 1549-3296. Available at: < http://dx.doi.org/10.1002/jbm.a.35325 >.

WANG, W.; YEUNG, K. W. K. Bone grafts and biomaterials substitutes for bone defect repair: A review. **Bioactive Materials,** v. 2, n. 4, p. 224-247, 2017/12/01/ 2017. ISSN 2452-199X. Available at: < http://www.sciencedirect.com/science/article/pii/S2452199X17300464 >.

WOOD, R. M.; MOORE, D. L. Grafting of the maxillary sinus with intraorally harvested autogenous bone prior to implant placement. **Int J Oral Maxillofac Implants,** v. 3, n. 3, p. 209-14, Fall 1988. ISSN 0882-2786 (Print) 0882-2786.

YUAN, H. et al. Osteoinductive ceramics as a synthetic alternative to autologous bone grafting. **Proc Natl Acad Sci U S A,** v. 107, n. 31, p. 13614-9, Aug 3 2010. ISSN 0027-8424.

ZHANG, D. et al. The development of collagen based composite scaffolds for bone regeneration. **Bioactive Materials,** v. 3, n. 1, p. 129-138, 2018/03/01/ 2018. ISSN 2452-199X. Available at: < http://www.sciencedirect.com/science/article/pii/S2452199X17300506 >.

APPENDIXES

DECLARATION OF EXCLUSIVE USE OF THE ARTICLE IN THESIS

We hereby declare that we are aware of the article **"Porous biphasic calcium phosphate ceramic for maxillary sinus floor augmentation: a randomized controlled clinical trial with CBCT, micro-CT and histomorphometry studies"** will be included in the Thesis of the student **Ricardo Quirico Pinheiro Machado** and was not used and may not be used in other works of Graduate Programs at the Bauru School of Dentistry, University of São Paulo.

Bauru, November 21, 2018

Ricardo Quírico Pinheiro Machado
Author — Signature

Ever Mena Laura
Author — Signature

Tania Mary Cestari
Author — Signature

Gerson Francisco de Assis
Author — Signature

Rumio Taga
Author — Signature

Marilia Afonso Rabelo Buzalaf
Author — Signature

DECLARATION OF EXCLUSIVE USE OF THE ARTICLE IN THESIS

We hereby declare that we are aware of the article **"Influence of biphasic calcium phosphate particle size on the repair of cranial critical-size bone defects"** will be included in the Thesis of the student **Ricardo Quirico Pinheiro Machado** and was not used and may not be used in other works of Graduate Programs at the Bauru School of Dentistry, University of São Paulo.

Bauru, November 21, 2018

Ricardo Quirico Pinheiro Machado
Author — Signature

Ever Mena Laura
Author — Signature

Tania Mary Cestari
Author — Signature

Ana Carolina Cestari Bighetti
Author — Signature

Ricardo Vinicius Nunes Arantes
Author — Signature

Nicole de Mello Carboni
Author — Signature

Bruna Carolina Costa
Author — Signature

Gerson Francisco de Assis
Author — Signature

Rumio Taga
Author — Signature

Marilia Afonso Rabelo Buzalaf
Author — Signature

ANNEXES

ANNEX

Approval of Ethical Committee

FACULDADE DE ODONTOLOGIA DE BAURU-USP

PARECER CONSUBSTANCIADO DO CEP

DADOS DO PROJETO DE PESQUISA

Título da Pesquisa: Avaliação Histológica e Histomorfométrica de um procedimento de elevação de seio maxilar utilizando uma cerâmica bifásica porosa: estudo clínico randomizado com avaliação após 4 meses de cicatrização

Pesquisador: Ricardo Quírico Pinheiro Machado

Área Temática:

Versão: 3

CAAE: 03525812.1.0000.5417

Instituição Proponente: Faculdade de Odontologia de Bauru-USP

DADOS DO PARECER

Número do Parecer: 139.405

Data da Relatoria: 31/10/2012

Apresentação do Projeto:

Trata-se de um projeto de mestrado com o título "AVALIAÇÃO HISTOLÓGICA E HISTOMORFOMÉTRICA DE UM PROCEDIMENTO DE ELEVAÇÃO DO SEIO MAXILAR UTILIZANDO UMA CERÂMICA BIFÁSICA POROSA: ESTUDO CLÍNICO RANDOMIZADO COM AVALIAÇÃO APÓS 4 MESES DE CICATRIZAÇÃO" de

autoria de Ricardo Quírico Pinheiro Machado sob a orientação da Profa. Dra. Marilia Afonso Rabelo Buzalaf.Para tal serão recrutados 36 pacientes, com idade entre 18 e 75 anos, com altura de osso alveolar menor que 5 mm na região mais estreita entre a parede do seio maxilar e a crista alveolar. Os 36 sujeitos da pesquisa serão aleatoriamente alocados em 3 grupos de tratamento (12/grupo) neste estudo clínico randomizado. A diferença entre os grupos será o tipo de material a ser utilizado para a elevação do seio maxilar, a saber: cerâmica bifásica porosa (experimental, HA+βTCP,Baumer S.A.), cerâmica bifásica comercial (GENPHOS, HA+βTCP,Baumer S.A.)ou osso autógeno. Quatro meses após a cirurgia, a formação do novo osso será avaliada através de tomografia computadorizada,bem como análises histológicas e histomorfométricas dos sítios de biópsias obtidas através da colocação dos implantes.O pesquisador pretende recrutar seus pacientes entre as pessoas que recorrerem à clínica de implantodontia da Associação Brasileira de Cirurgiões Dentistas de Balneário Camboriú, Santa Catarina, nos anos de 2012 e 2013, para reabilitação protética unilateral de suas regiões maxilares parcialmente edentulas.

Endereço: DOUTOR OCTAVIO PINHEIRO BRISOLLA 75 QUADRA 9
Bairro: VILA NOVA CIDADE UNIVERSITARIA **CEP:** 17.012-901
UF: SP **Município:** BAURU
Telefone: (14)3235-8356 **Fax:** (14)3235-8356 **E-mail:** mferrari@fob.usp.br

FACULDADE DE ODONTOLOGIA DE BAURU-USP

Objetivo da Pesquisa:

Esta pesquisa tem por objetivo testar a hipótese nula de que a utilização de uma cerâmica bifásica porosa não terá efeito significativo na formação de novo osso 4 meses após a elevação da parede do seio maxilar, em comparação à cerâmica bifásica densa (GENPHOS, Baumer S.A.) e ao osso autógeno.

Avaliação dos Riscos e Benefícios:

Riscos: O estudo oferece certo risco ou desconforto aos participantes, uma vez que os procedimentos realizados serão cirúrgicos. Os riscos não devem ultrapassar uma normalidade dentro das cirurgias orais deste tipo. Pode-se esperar desconfortos pós operatórios, tais como: dor leve e moderada nos primeiros dias,abertura da sutura (pontos), sangramento moderado, edema (inchaço) localizado. Segundo o autor da pesquisa, todo voluntário terá o acompanhamento necessário no pré e pós operatório.

Benefícios: Segundo o autor da pesquisa, através dos resultados desta pesquisa, saber-se-á a quantidade e qualidade do novo osso formado, bem como a ausência ou não de inflamações teciduais. A coleta intrabucal de enxerto de osso autógeno pode levar à morbidade do sítio doador e prolongar o tempo cirúrgico, além de prover material de enxerto em quantidade limitada. Além disto, quando utilizado como um enxerto onlay, o osso

esponjoso autógeno de origem extrabucal sofre reabsorção, o que resulta em mínimo ganho ósseo. Com a utilização dos biomateriais pretende-se minimizar esta morbidade da regiao doadora e a quantidade do material para enxertia pode ser obtido tanto quanto necessário.

Comentários e Considerações sobre a Pesquisa:

Trata-se de um estudo clínico randomizado que irá testar a utilização de uma cerâmica bifásica porosa e se utilizará de 36 voluntários. Os voluntários não saberão o tipo de tratamento ao qual serão submetidos de modo que o estudo será conduzido de maneira triplo-cega. Todos os voluntários se submetrão a tomadas radiográficas, sofrerão intervenções cirúrgicas e alguns desconfortos. Sendo do conhecimento deles todos os

procedimentos a que serão submetidos, não existe problema ético que inviabilize a pesquisa.

Considerações sobre os Termos de apresentação obrigatória:

Todos os documentos e explicações solicitadas para análise desta pesquisa foram devidamente encaminhados pelos pesquisadores.

Recomendações:

Não há.

Conclusões ou Pendências e Lista de Inadequações:

Depois de exclarecidas todas as pendências, apresentados todos os documentos necessários para análise, com a devidas adequações, sou de parecer que o projeto possa ser aprovado.

Endereço: DOUTOR OCTAVIO PINHEIRO BRISOLLA 75 QUADRA 9
Bairro: VILA NOVA CIDADE UNIVERSITARIA **CEP:** 17.012-901
UF: SP **Município:** BAURU
Telefone: (14)3235-8356 **Fax:** (14)3235-8356 **E-mail:** mferrari@fob.usp.br

FACULDADE DE ODONTOLOGIA DE BAURU-USP

Situação do Parecer:

Aprovado

Necessita Apreciação da CONEP:

Não

Considerações Finais a critério do CEP:

O CEP acata o parecer APROVADO emitido pelo relator.

Esse projeto foi considerado APROVADO. O CEP-FOB/USP exige a apresentação de relatórios anuais (parciais e finais), conforme o cronograma apresentado. Qualquer alteração na metodologia e/ou título e a inclusão ou exclusão de autores deverá ser prontamente comunicada. Lembramos que na apresentação do relatório final, deverão ser incluídos todos os TCLEs e/ou termos de doação de dentes devidamente assinados e rubricados.

BAURU, 06 de Novembro de 2012

Assinador por:
Maria Teresa Atta
(Coordenador)

Endereço: DOUTOR OCTAVIO PINHEIRO BRISOLLA 75 QUADRA 9
Bairro: VILA NOVA CIDADE UNIVERSITARIA **CEP:** 17.012-901
UF: SP **Município:** BAURU
Telefone: (14)3235-8356 **Fax:** (14)3235-8356 **E-mail:** mferrari@fob.usp.br